5-2015

Development and Evaluation of a Cost Effective Plant Growth Media Moisture Sensor and Development of an Aqueous Data Transmission System for Irrigation Purposes

Steven Michael Pickett
University of Tennessee - Knoxville, spicket1@vols.utk.edu

To the Graduate Council:

I am submitting herewith a thesis written by Steven Michael Pickett entitled "Development and Evaluation of a Cost Effective Plant Growth Media Moisture Sensor and Development of an Aqueous Data Transmission System for Irrigation Purposes." I have examined the final electronic copy of this thesis for form and content and recommend that it be accepted in partial fulfillment of the requirements for the degree of Master of Science, with a major in Biosystems Engineering.

John B. Wilkerson, Major Professor

We have read this thesis and recommend its acceptance:

John R. Buchanan, Kimberly D. Gwinn

Accepted for the Council:
Dixie L. Thompson

Vice Provost and Dean of the Graduate School

(Original signatures are on file with official student records.)

Development and Evaluation of a Cost Effective Plant Growth Media Moisture Sensor and Development of an Aqueous Data Transmission System for Irrigation Purposes

A Thesis Presented for the
Master of Science
Degree
The University of Tennessee, Knoxville

Steven Michael Pickett
May 2015

DEDICATION

I would like to dedicate this thesis to my parents, Paul and Emilia Pickett, and my brother, Neil Pickett, for all of your love and encouragement throughout my education. I am thankful every day for the life you have given me. I would also like to dedicate this to a special friend and her family, who spent a lot of time and effort pushing me to get through school even when I didn't believe it was possible. All of you have invested in me and I can only hope to pass that along in the future. Thank you.

ACKNOWLEDGEMENTS

I would like to thank my advisor and committee, Dr. John Wilkerson, Dr. John Buchanan, and Dr. Kimberly Gwinn for getting together and making this research project a reality. I would also like to thank David Smith for being a sounding board for my ideas, even when they were off the wall, and providing invaluable advice and expertise when needed.

ABSTRACT

The ability to accurately monitor and transit the moisture content of soilless growing media in the rooting zone is critical for plant-based research, production of high value crops, and other agricultural production. The focus of this study is the development and evaluation of a cost effective moisture sensor designed to measure the plant-available moisture content of growing media and the development of a aqueous data transmission method for relaying this information back to a central location. While there are currently many commercially available soil moisture sensors on the market, the aim of this research is not to develop a more accurate sensor but to design a comparably capable sensor that is more cost effective for the end user to achieve a higher spatial resolution of their moisture measurement by incorporating more sensors over a given area. Traditional wired and wireless communication methods currently used in industry would require additional infrastructure to transmit this moisture data back to central local that adds to the cost of the system. The proposed aqueous data transmission system was designed to relay moisture sensor output utilizing the existing irrigation infrastructure for communication. This system, if commercialized, could improve currently employed automated irrigation for production systems by optimizing water management based on zone requirements, thereby increasing production efficiency while minimizing the potential for off-site movement of contaminates. Likewise, this low cost approach will allow a network of soil moisture sensors to address the spatial variation of moisture content within an area; thus permitting site-specific irrigation within a production area (field, greenhouse etc).

TABLE OF CONTENTS

LIST OF TABLES

LIST OF FIGURES

INTRODUCTION

Increased demand for water resources and stricter regulations make it essential to improve the efficacy and cost of agricultural water usage. Agriculture expends the majority of the nation's water supply for the production of food and feed. As the awareness of these two facts has become more and more prevalent, there has been a concentrated effort in the application of water management to improve efficiency through the implementation of new techniques and systems designed to reduce water usage (Christian-Smith and Gleick, 2012). Drip irrigation and other site-specific irrigation methods are among the methods to improve efficiency, but these systems often rely on a fixed flow rate for a specific amount of time per day rather than taking into account water requirements (Nemali and van Iersel, 2006). Automation of these systems based on actual water requirement offers an improved method to further increase irrigation efficiency.

Water requirement in plants can vary from plant to plant based on environmental conditions, plant health, and plant maturity. Current irrigation methods overlook this fact and irrigate regardless of need, causing increased fertilizer mobilization and increased irrigation cost. If the water requirement of a particular zone can be determined, these costly shortcomings can be reduced by matching irrigation to the needs of plants in that zone. As the price of moisture sensors goes down, the possibility of providing irrigation based on site specific needs becomes a more plausible possibility.

Irrigation based on water requirements is predicated on the ability to sense zonal plant growth media moisture content and relaying that information to a centralized location in order to make the decision to irrigate or not. Chapter 1 of this thesis goes into the detail of the development and evaluation of a sensor capable of sensing moisture content. Chapter 2 describes a method of transmitting this data via the waterline back to a centralized location upstream from the point of irrigation.

CHAPTER I

Development and Evaluation of a Cost Effective Plant Growth Media Moisture Sensor

Abstract

The ability to accurately monitor the moisture content of soilless growing media in the rooting zone is critical for plant based research, production of high value crops, and other plant-based agricultural production systems. The focus of this study is the development and evaluation of a cost effective moisture sensor designed to measure plant-available moisture content of growing media. While there are currently many commercially available soil moisture sensors on the market, the aim of this research is not to develop a more accurate sensor but to design a comparably capable sensor that is more cost effective for the end user to achieve a higher spatial resolution of their moisture measurement by incorporating more sensors over a given area. The sensor makes use of capacitance phenomenon to detect changes in dielectric properties of the wetted media in close proximity to the sensor. Finite element difference was used to model the electric field of several potential planar-coaxial geometry variations. These simulations were performed to find geometries that maximized the electric field cast into the wetted media while minimizing effects of potential air gaps at that media-sensor interface. A series of sensor electrode geometries were then constructed using standard rapid printed circuit board (PCB) prototyping techniques. Measurement of sensor accuracy was assessed by comparing gravimetrically-determined moisture content with prototyped sensors and a commonly used commercially available technology. This sensor, if commercialized, could improve currently employed automated irrigation for production systems by optimizing water management based on zone requirements, thereby increasing production efficiency while minimizing the potential for off-site movement of contaminates. Likewise, this low cost approach will allow a network of

soil moisture sensors to address the spatial variation of moisture content within an area; thus permitting site-specific irrigation within a production system based on zone requirements. An additional benefit, researchers and producers will be able to explore different possibilities in data-mining as well as the possibility of developing historical models for disease outbreaks, yield, and irrigation requirements by compiling sensor data over time. These models will benefit from the increased spatial resolution afforded by a lower cost alternative to currently available commercial sensors.

Introduction

Soil moisture is an important variable to measure for more than just agricultural reasons. The plant disease triangle is a well-known illustration (figure 1) of the simplest ways to minimize the risk of disease outbreak. One side of the triangle is dedicated to the environment around the plant. These environmental factors include soil moisture and several other moisture related factors like relative humidity, standing water, and leaf wetness. In order to have disease, all three sides must be present (Krupinsky et al., 2002). Sensing soil moisture makes it possible to monitor a portion of the environmental factor of the triangle. The effects and interactions of soil moisture have been researched thoroughly on a range of plants and pathogens. These include:

- soil moisture stress on barley (Aspinall et al., 1964),
- soil moisture stress on different growth stages of corn (Denmead and Shaw, 1960),
- root rot and wilt of chickpeas (Bhatti and Kraft, 1992), and
- pink root of onion cultivars (Coleman et al., 1992) and various other academic studies.

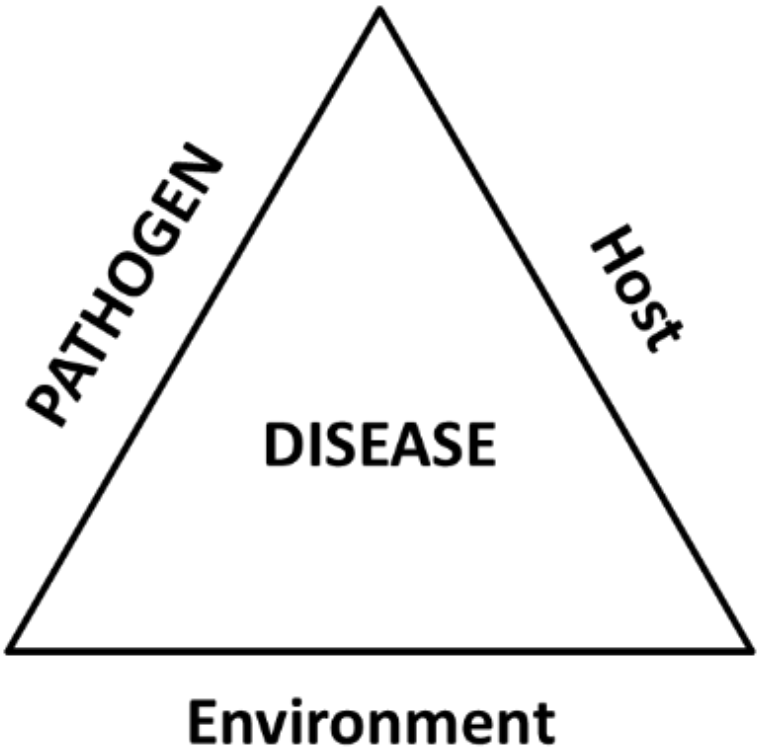

Figure 1: Illustration of the disease triangle. All three factors (host, pathogen, and environment) of the triangle must be present for there to be potential for disease. Soil moisture is one part of the environmental factor.

The disease triangle is applicable to plants, humans, and animals as well. By sensing soil moisture, it is possible to predict the transmission factors of malaria according to Patz (1998). Increased soil moisture provides a breeding ground for mosquitoes which are a transmission vector of malaria. The World Health Organization estimated that malaria caused as many as 750,000 deaths worldwide in 2012 (WHO, 2013).

Objective

There are different methods to measure soil moisture that range in complexity, accuracy, and cost. These methods include neutron scattering, gamma attenuation, and nuclear magnetic resonance. While accurate, these techniques are costly and often difficult to perform *in situ*. Other methods such as electrical resistive, tensiometric, thermal, and hygrometric techniques are less costly but are subject to other drawbacks including: extensive calibration or increasing error over time (Zazueta and Xin, 1994). A capacitive approach was chosen based on its cost, accuracy, and ability to be remotely implemented. The goals of this study were:

i. To develop a low-cost, minimally-intrusive capacitive sensor for remote measuring of rooting zone moisture content of soilless growing media,
ii. To evaluate the potential of measuring changes in electrical AC properties to model moisture content, and
iii. To produce a model relating capacitance of the sensor to gravimetric moisture content of the selected test media.

Background

Measurement of soil moisture is not a new idea, and there are multiple successfully derived methods to quantify this variable. Each of the currently used methods differ in complexity, accuracy and cost; this paper specifically refers to the use of capacitance to measure soil moisture. Zazueta and Xin (1994) give brief descriptions of a broad range of methods while giving the advantages and disadvantages of each. The different techniques can be categorized in three broad classifications; destructive or non-intrusive, inexpensive or costly, complicated or simple. More specifically they can be classified in one of three major techniques employed to measure the moisture content of the soil: gravimetric, nuclear, and electromagnetic. Capacitive sensing methods fall into the electromagnetic category.

Gravimetric and nuclear techniques make up a large portion of the methods commonly used. They are poor choices for remote sensing applications but are still worthwhile to include brief descriptions of each for elucidative purposes. The most used method is a gravimetric technique referred to as the oven-dried soil moisture content measurement. Gravimetric techniques are typically destructive, simple, relatively inexpensive, and accurate, but gravimetric techniques are often time consuming and hard to implement as automated measurements in the field. Nuclear techniques on the other hand are generally complicated, expensive, and require radioactive sources, but they are highly accurate, non-intrusive and have a much lower response time compared to gravimetric techniques.

Electromagnetic techniques take advantage of either resistive or capacitive properties to measure moisture. This refers to the specific way the measurement is taken and what electromagnetic theory it relies on. Impedance is made up of a real component (resistance) and an imaginary component (capacitance) (Sadiku, 2014). Sensors designed to measure the real component rely on a changes in resistance between two stationary probes to determine the moisture content. This measurement is strongly influenced by pH and salinity as they alter the electrical resistivity of the water. Capacitive sensors utilize the imaginary component of impedance and measure changes in the dielectric properties of the material. While measuring the imaginary component is often more complicated and expensive than measuring the real component, it provides a measurement that minimizes the influences of salinity and temperature. Zazueta and Xin (1994) describe the capacitive soil moisture sensor as having the advantage of being able to take an instantaneous measurement of soil from which the absolute soil moisture can potentially be derived. The cost and long term stability of this sensor are credited as being disadvantages of this technique; however, this concern has diminished with advancements in industrial electronics.

Gravimetric, nuclear, and electromagnetic techniques have been used to develop soil moisture sensors in the past. Each method has its advantages and disadvantages such as cost, complexity, and ability to be implemented remotely. Gravimetric techniques are simple, accurate, time consuming and hard to implement remotely. Nuclear techniques are accurate methods for detecting soil moisture, but are cost prohibitive. Electromagnetic techniques are ideal for implementing remotely, but resistive methods depend strongly on temperature and salinity of the

soil. The majority of capacitance sensor research conducted previously is based on parallel plate theory to measure soil moisture. Thin film coaxial geometries, compared with parallel plate capacitors, offer a more simplistic manufacturing process and can be incorporated into a PCB layout. This design was ultimately chosen for its simplicity, cost, and ease of remote implementation.

Dean et al. (1987) reported their capacitive soil moisture sensor as being able to detect a change in soil moisture of 0.02% by volume. This is due to the dielectric constant of soil being approximately 4, while the dielectric constant of water is approximately 80 (Hasted, 1973). Using linear regression, Whalley et al. (1992) found that 84% of variation in output frequency of their sensor could be explained by the water content of the sample soil. Both Dean et al. (1987) and Whalley et al. (1992) used the same sensor configuration that resembles the typical parallel plate capacitor used to model capacitance. Figure 2 demonstrations this configuration with equation 1 describing the relationship between the shown variables.

The equation for calculating parallel plate capacitance is as follows:

$$C = \varepsilon_0 k \frac{A}{d} \quad (1)$$

where
C = Capacitance (F)
ε_0 = Permittivity of free space (F m^{-1})
k = Dimensionless dielectric constant
A = Area of the plate (m^2)
d = Distance between plates (m)

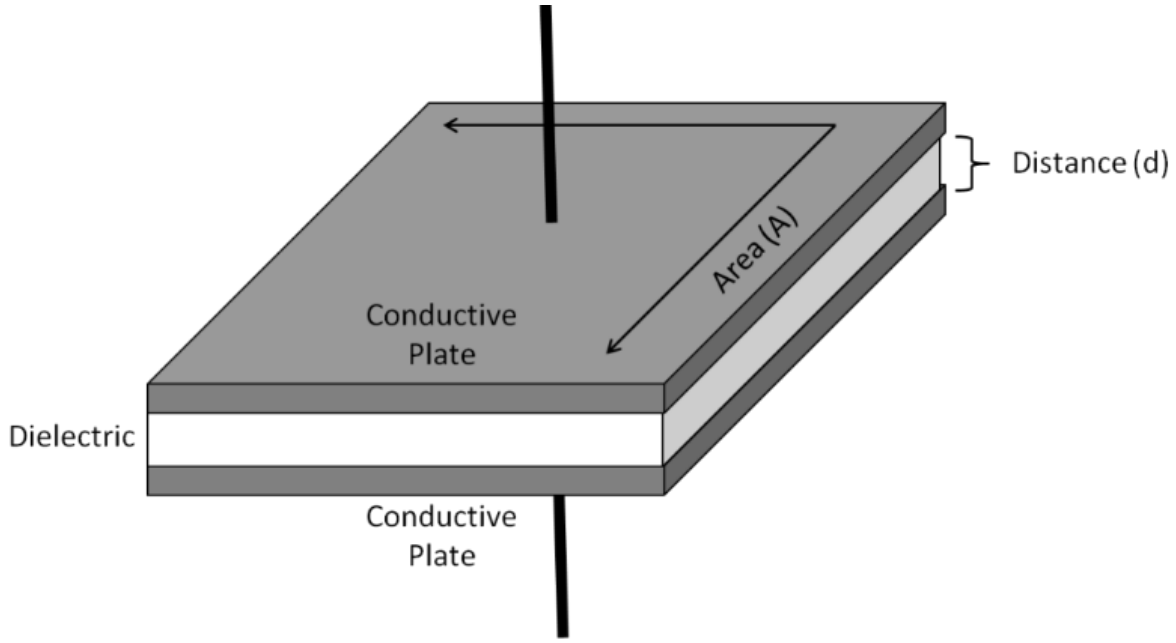

Figure 2: Illustration of the basic configuration for a parallel plate capacitor. Two conductive plates are separated by a non-conductive material. Parallel plate capacitors can take many forms other than the simplified illustration shown here.

The dielectric material between two plates creates an electrical field proportional to the electric potential between the plates and inversely proportional to the distance between the plates. A cylindrical design has the conductive plates side by side in the same plane rather than opposing each other (figure 3). This type of design is conducive to being mass produced as a simple, a single-sided printed circuit board (PCB). It also has the advantage of causing the electrical field to potentially extend farther away from the surface of the capacitor.

The equation for calculating coaxial capacitance (*C*)follows:

$$C = \frac{2\pi\varepsilon_0 kL}{\ln(\frac{b}{a})} \qquad (2)$$

where
L = length of the cylinder (m) – shown going into the page
a = radius of the inner plate (m)
b = radius to the foremost edge of the outside outer plate (m)
ε_0 = Permittivity of free space (F m^{-1})
k = Dimensionless dielectric constant

The application of this formula (equation 2) stipulates that L must be much larger than b. For the purposes of this study, the dimension of L is small compared to both the pad dimension as well as the b dimension to the inner edge of the outer pad. Therefore, equation 2 is not directly applicable to the proposed sensor where L would be the thickness of the copper clad. In order to quantify the potential for capacitance, the electric field density can be modeled using finite difference method. Using equation 3, it is possible to iteratively calculate the voltage potential of any given point by averaging the neighboring points.

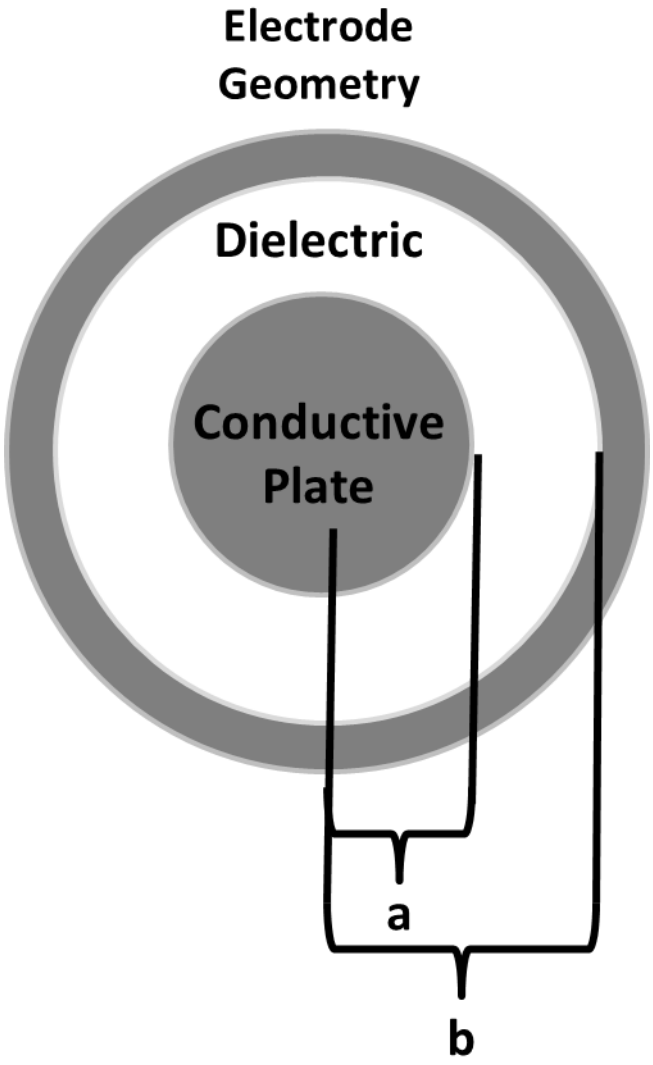

Figure 3: Illustration of a coaxial capacitor geometry. The radial dimension of the inner pad is represented by **a**, and **b** is the radial dimension to the foremost edge of the outside pad.

$$V_{i,j} = \frac{1}{4}\left(V_{i+1,j} + V_{i-1,j} + V_{i,j+1} + V_{i,j-1}\right) \quad (3)$$

where
$V_{i,j}$ = The voltage potential of a chosen point
$V_{i+1,j}$ = The voltage potential to the right of the chosen point
$V_{i-1,j}$ = The voltage potential to the left of the chosen point
$V_{i,j+1}$ = The voltage potential above the chosen point
$V_{i,j-1}$ = The voltage potential below chosen point

Design Approach

Initial design efforts focused on the selection of which physical phenomenon to use for determining soil moisture. Studies comparing currently available methods for determining soil moisture may be found in Walker et al. (2004); Leib et al. (2003). The sensing techniques used in these studies were either too costly or have electrical power requirements not suitable for the purpose of remote wireless sensing technology. Thermal and electromagnetic methods are both cost effective options. Sherfy (2008) details the construction and evaluation of a thermal sensor probe with the capability to determine water content, electrical conductivity and several thermal properties of soil. Thermal sensing techniques rely on an artificial heat source to measure thermal conductivity in order to estimate water content. Due to the increased power consumption that thermal conductance measuring techniques require, they were abandoned as design options. Comparatively, electromagnetic methods tend to be easily implemented remotely and have low power requirements.

Electromagnetic techniques employ the use of resistance, capacitance, or a combination of the two in order to determine soil moisture. Resistive techniques use sensor probes, often encased in gypsum, to measure electrical conductivity. These sensors are prone to degradation when operated with direct current due to the effects of electrolysis. This can be mitigated by using an alternating current signal instead, but this adds complexity to the circuitry. Another drawback to using resistive techniques is that resistance is highly dependent on ionic content as well as temperature and requires recalibration over time (Zazueta and Xin, 1994). The effects of these issues can also be lessened by normalizing data and adding temperature into the prediction model. This adds more complexity to the system and additional avenues for error. Capacitance is determined by the surface area of two plates separated by a given space with certain dielectric properties. By forcing all variables to be constant with the exception of the interplatal dielectric constant, it is possible to relate capacitance to a mixture of two substances with differing dielectric constants (soil $\varepsilon \approx 4$; water $\varepsilon \approx 80$) (Hasted, 1973). Using capacitance to determine moisture is attractive because of its relative ease of construction and minimizes the negative effects due to salinity and temperature. For these reasons a capacitive approach was chosen.

In recent years, there has been a strong push in the sensor industry to integrate data acquisition systems into the embodiment of the senor. This minimalizes cost and decreases the design cycle time required for new development. These sensors are referred to as mixed signal devices or smart sensors. Combining these two realms into a mixed signal device achieves two objectives: 1) it keeps analog lines as short as possible with minimal connections, which shields them from

interference and noise; and 2) it speeds up the prototyping stage by allowing design engineers to directly interface with the sensor digitally through a microcontroller rather than having to construct amplification and/or analog to digital conversion circuitry. A mixed signal device built on a PCB substrate was chosen to construct the mixed signal sensor due to its flexibility and ability to be inexpensively mass produced upon final design, meeting the criteria detailed in objective (i).

Designing the sensor based on parallel plate capacitor design was rejected for the fact that measuring soil moisture between two plates was deemed to not be plausible. A geometry that utilized a single plane for both plates was chosen in order to extend the electrical field into the sensed material and to allow for the use of a single PCB for construction. Theoretical calculation of the capacitance in a single planar design becomes difficult due to edge effects of the electrical field so finite element difference (FED) was used to estimate the potential performance of several geometries before one was selected for prototyping and testing.

Visualization of the electrical field produced by a specific design was possible using FED. This allowed for the direct comparison of field intensity at different critical points in space. Edge effects are the main component in the determination of capacitance of a signal planar geometry based capacitor. As the gap between the two plates gets smaller the electrical field become more intense and concentrates closer to the surface of the sensor. As the distance between the two plates decreases, the electrical field becomes more intense and is increasingly influenced by the

sensed material. This relationship can be seen in FED models. Several variations of the prototype geometry were selected to analyze the overall influence of this phenomenon.

Materials and Methods

Sensor design was the first step in the three part process. It was possible to develop a potential sensor design by applying the theory of capacitance to a physical design that measured a change in the dielectric properties of a material. Finite difference method was used to simulate the electric field density of a radial coaxial plate capacitor. Ranganath (2013) MATLAB FED parallel plate simulation program was modified to simulate the cross sectional electrical field of a thin coaxial capacitor. The modified code can be found in appendix A. The results of this simulation comparing two different sensor prototypes with different inner and outer conductor dimensions is illustrated in figure 4. Simulation aided in the design of several prototype sensors capable of measuring soil moisture. A series of prototypes with varying physical pad dimensions (a and b dimensions seen in figure 3) were developed and constructed so that initial testing could be performed to determine what, if any, differences these minute variations made. This was done in order to select a geometry that maximized the performance of the moisture measurement. Different potential sensors designs were briefly compared using measurements taken using a LCR meter (inductance, capacitance, and resistance) to measure the capacitance and, total impedance (Z) of a wetted media. The best performing geometry was then selected for more extensive testing.

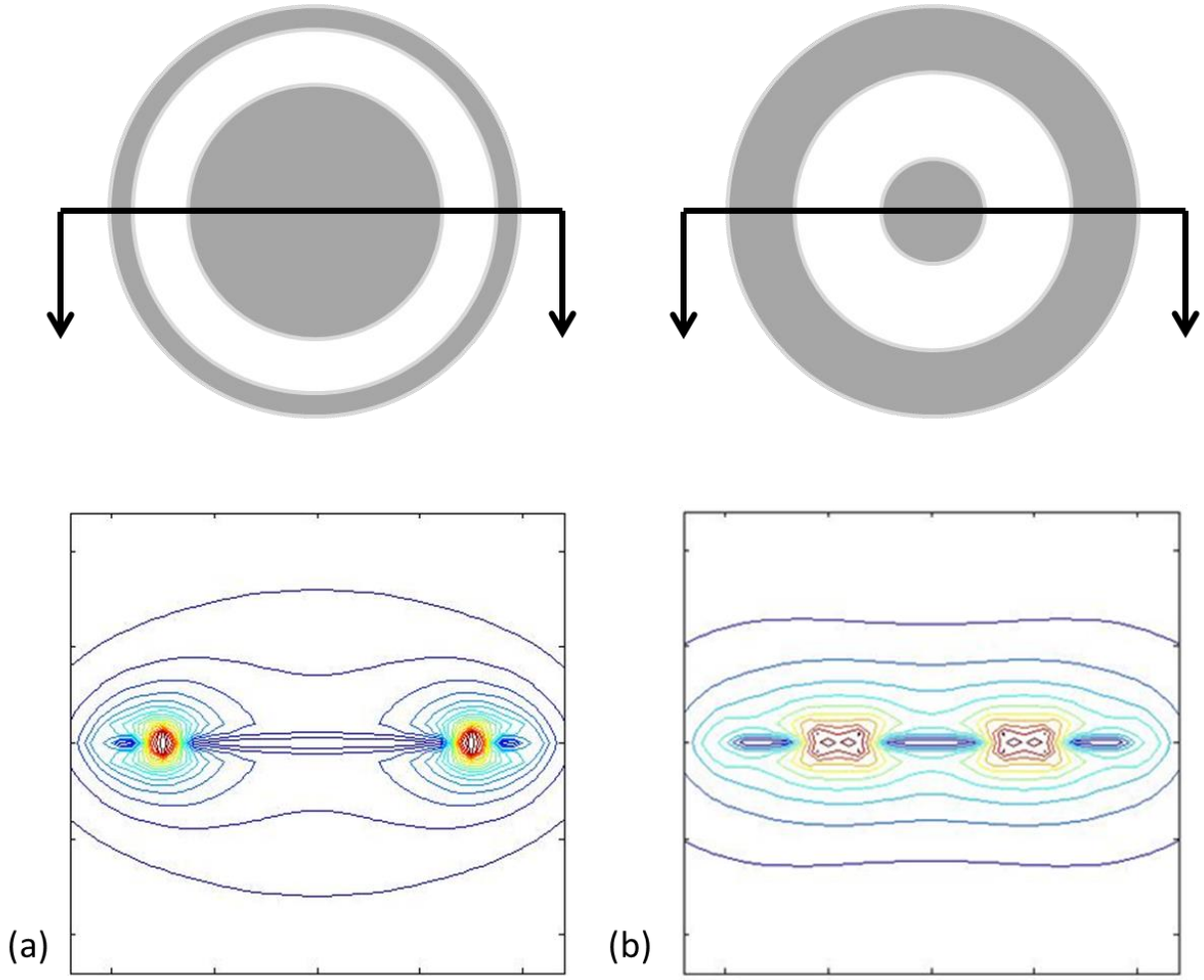

Figure 4: Finite element difference simulated cross section of electrical field showing relative intensities. (a) Electric field produced from a sensor with a small outer pad width, large inner pad width, and medium gap between. The electrical field is highly concentrated in the gap between pads; (b) Electric field produced from a sensor with medium outer pad width, medium inner pad width, and medium gap between. The electrical field is less intense comparatively and covers a larger area.

Verification, calibration, and validation demonstrated the efficacy of this sensor and allowed for further improvement upon the initial design. Comparison of moisture content measurements to data from Watermark sensors verified that the sensor was, in fact, measuring the moisture content while making it possible for calibrations and other iterative improvements to be made. During this phase of the project, an accuracy assessment of both the proposed sensor and a Watermark sensor data was conducted using controlled conditions to evaluate the performance of the proposed sensor. Small scale testing using soilless growing media was performed to demonstrate the final design and to gather information about how the sensor faired real world environment. Two sensors were placed at uniform depths to collect soil moisture data over several wetting cycles in the environmental chamber. A Watermark soil moisture sensor was included in testing for validation.

Experimental Design

Sensors were evaluated using two different wetted media. Household cellulose sponges made from wood pulp were used for the purpose of lab testing. This eliminated influences of non-homogenous media on the dielectric constant. Validation of the sensors was then tested in a second media using a blended soilless growing media similar to what is commonly used in greenhouses.

Each prototype was inserted between two cellulose sponges (figure 5a, 5b) to create a uniform experimental unit (EU) and placed inside of an environmental chamber (Cincinnati Sub-Zero model Z16+) as presented in figure 5c. Experimental units were saturated prior to testing.

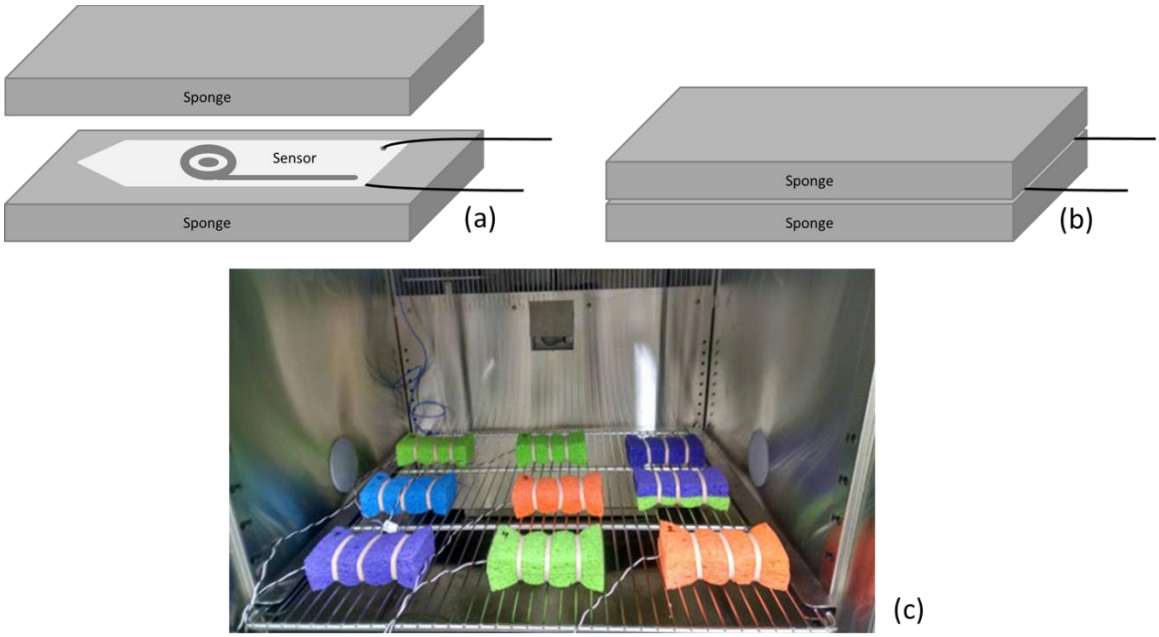

Figure 5: (a) Illustration of an expanded experimental unit comprised of two cellulose wood pulp sponges and a sensor; (b) Illustration of an assembled experimental unit; (c) Several experimental units prepared for environmental chamber testing.

Temperature was held constant throughout each test. Spacing between each EU was held constant in order to minimize variations in evaporation rates. As moisture content decreased, measurements of capacitance for each sensor were taken using a QuadTech RLC meter (model 7600B) connected to a PC for data logging purposes. Water content of each EU was calculated gravimetrically by weighing the EU for each capacitance measurement.

Methods

Sensors were constructed by milling FR-4 printed circuit board substrate to minimize cost and meet objective (i). To study the second objective, sensors with varying inner and outer pad dimensions (figure 6) were manufactured in-house and subjected to the following experimental procedure.

Each EU was initially saturated and placed into the environmental chamber at a set temperature and relative humidity (RH). Moisture was removed by varying RH in order to increase or decrease the rate of moisture removal over the period of a week or until the moisture content of the EUs was below 25% (w/w). This procedure was performed at 20˚C, 25˚C and 30˚C in order to quantify the influence of temperature on the capacitance measurements. During the day, RH was decreased to approximately 60% in order to increase the rate of moisture removal and measurements were taken every two hours; at night RH was increased to approximately 90% to minimize the change in moisture content of the EUs when measurements were not taken. RH and temperature conditions that caused condensation in the environmental chamber were avoided because it disturbed the moisture profile of the EU temporarily. Moisture content measurements,

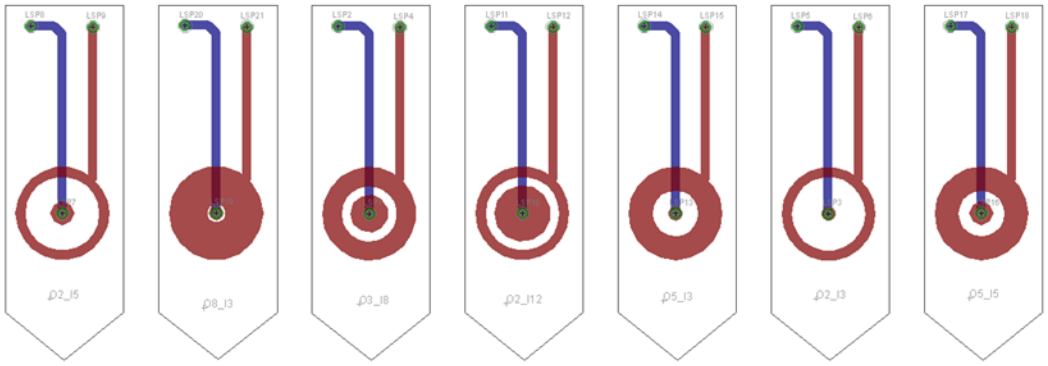

Sensor	Inner pad diameter (mm)	Outer Pad Width (mm)	Overall Width (mm)
1	5	2	25
2	3	8	25
3	8	4	25
4	12	2	25
5	3	5	25
6	3	2	25
7	5	5	25

Figure 6: Illustration of the 7 geometries used to construct PCB based prototype sensors. CadSoft Eagle was used to design the geometries with varying pad dimensions listed above to determine what relationship these variations had on performance of the prototype sensors.

gravimetric and volumetric, assume that moisture is evenly distributed throughout the material. This is not true due to the convective nature of evaporation and can drastically effect capacitance measurements based on the moisture profile. A moisture gradient is quickly developed due to this and is unavoidably built into the resulting model.

Measurements

Each of the seven EUs were removed from the environmental chamber and measured for parallel capacitance and impedance using the LCR meter over 25 frequencies ranging from 500Hz to 5kHz. This frequency range was selected based on initial frequency sweeps taken to determine the capacitive response over a much larger frequency range. Frequencies below 500 Hz had a greater change in capacitance due to changes in moisture content but were observed to have a higher degree of noise. Frequencies greater than 5 kHz had a much smaller change in capacitance due to changes in moisture content. The AC signal was set to 1Vp-p. LCR measurements were performed in triplicate and averaged. Data were transmitted serially to a connected PC. EU weight was measured and recorded manually in order to calculate gravimetric moisture content. Figure 7 illustrates the measurement area.

Results and Discussion

Environmental chamber tests were conducted on each of the seven sensors at three different temperatures (20˚C, 25˚C, 30˚C) over a range of moisture contents (90% to 20%) and 25 signal frequencies (500 Hz to 5 kHz). The sensors were placed between household sponges to simulate a wetted media for testing. Figure 8 illustrates the relationship between environmental and

Figure 7: Photograph of the environmental testing chamber and LRC meter setup for data gathering.

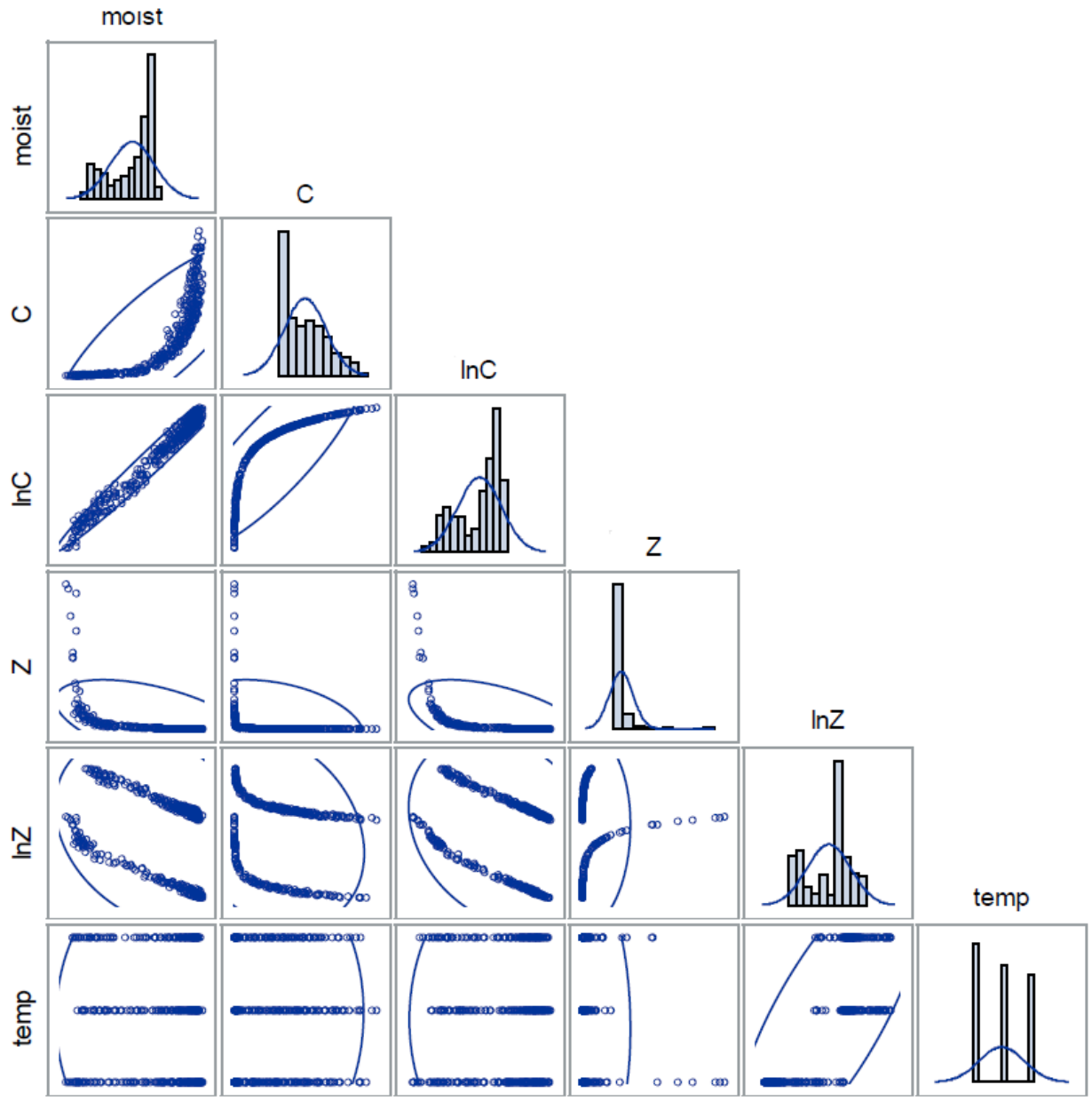

Figure 8: Correlation analysis (performed in SAS 9.3) illustrating the relationship between environmental and electrical attributes (moisture, capacitance, natural log of capacitance, impedance, natural log of impedance, and temperature.) A strong linear relationship between moisture and natural log of capacitance is indicated by the grouping shown.

electrical attributes with a correlation analysis (SAS 9.3, Cary NC) that was performed on the measured variables (capacitance and total impedance) and their log transformations to determine which variable had a linear relationship with moisture content. A strong logarithmic trend was observed in the LCR meter capacitance output. An example of this can be seen in output from prototype 4 (figure 9). Output data was transformed for SAS analysis by taking the natural log of the LCR capacitance output to build a model to linearly predict moisture. A simple linear regression model was used (SAS 9.3, Cary NC) to determine if the log transformation of measured capacitance taken using the prototype sensors could be modeled to predict moisture content at a single frequency as well as over several frequencies. Error increases with increases in test signal frequency (table 1). This was observed for each of the prototypes. For this reason, a 500 Hz signal was used for the signal frequency. Regardless of sensor geometry, 97% of the moisture differences could be explained by differences in capacitance ($P<0.001$) with a root mean square error (RMSE) of 4.0% moisture. Prototype 1 and 4 individually performed the best of the different geometries, explaining 99% of the moisture differences by differences in capacitance ($P<0.001$) with RMSE of 2.2% moisture for both sensors. Prototype 6 and 7 were the lowest performing sensors, explaining 98% of the moisture differences by differences in capacitance ($P<0.001$) with RMSE of 3.8% moisture for both prototypes.

Sensor output showed a clear trend between prototypes. The generic model (figure 10) resulted in a higher RMSE than any of the specific individual sensor models but would still be capable of reasonably predicting moisture content categorically (saturated, wet, dry, needs irrigation, etc.)

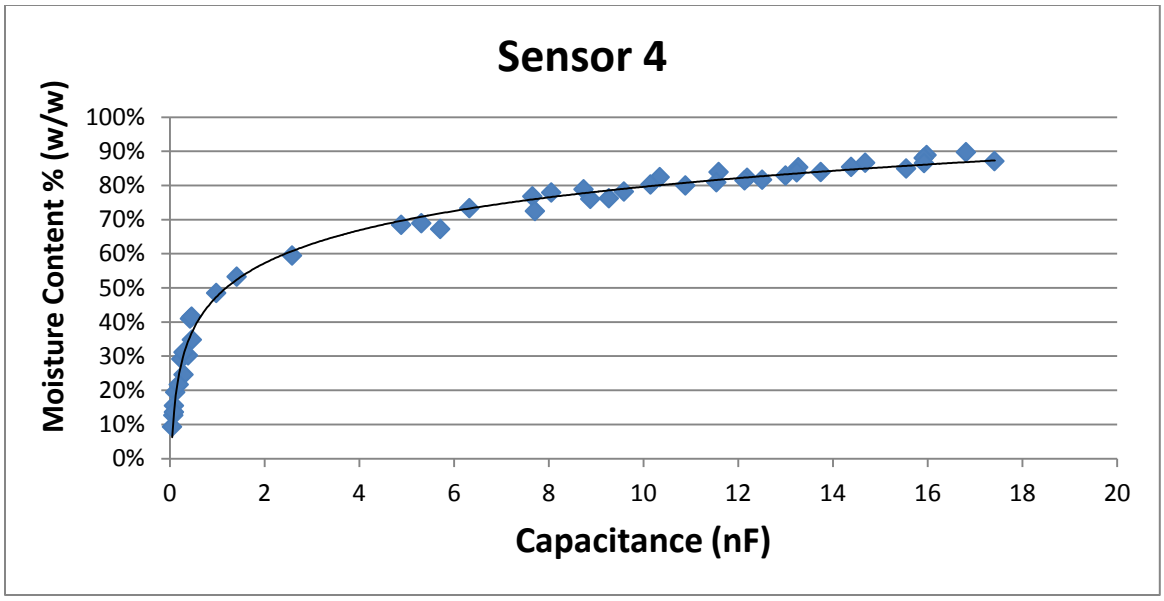

Figure 9: Untransformed output relating moisture content vs. capacitance of prototype sensor 4. A strong logarithmic trend in the data is apparent from the graph.

Table 1: Models created with data collected using higher frequency signals exhibited a decreasing relationship with performance.

	Frequency (Hz)	RMSE (% moisture)	R^2	95% Prediction Limits (% moisture)
Prototype 1	500.0	2.27%	0.994	4.53%
	733.8	2.70%	0.992	5.40%
	1077.2	3.45%	0.987	6.90%
	1581.1	4.30%	0.979	8.61%
	2320.7	5.25%	0.969	10.50%
	3406.4	6.28%	0.956	12.57%

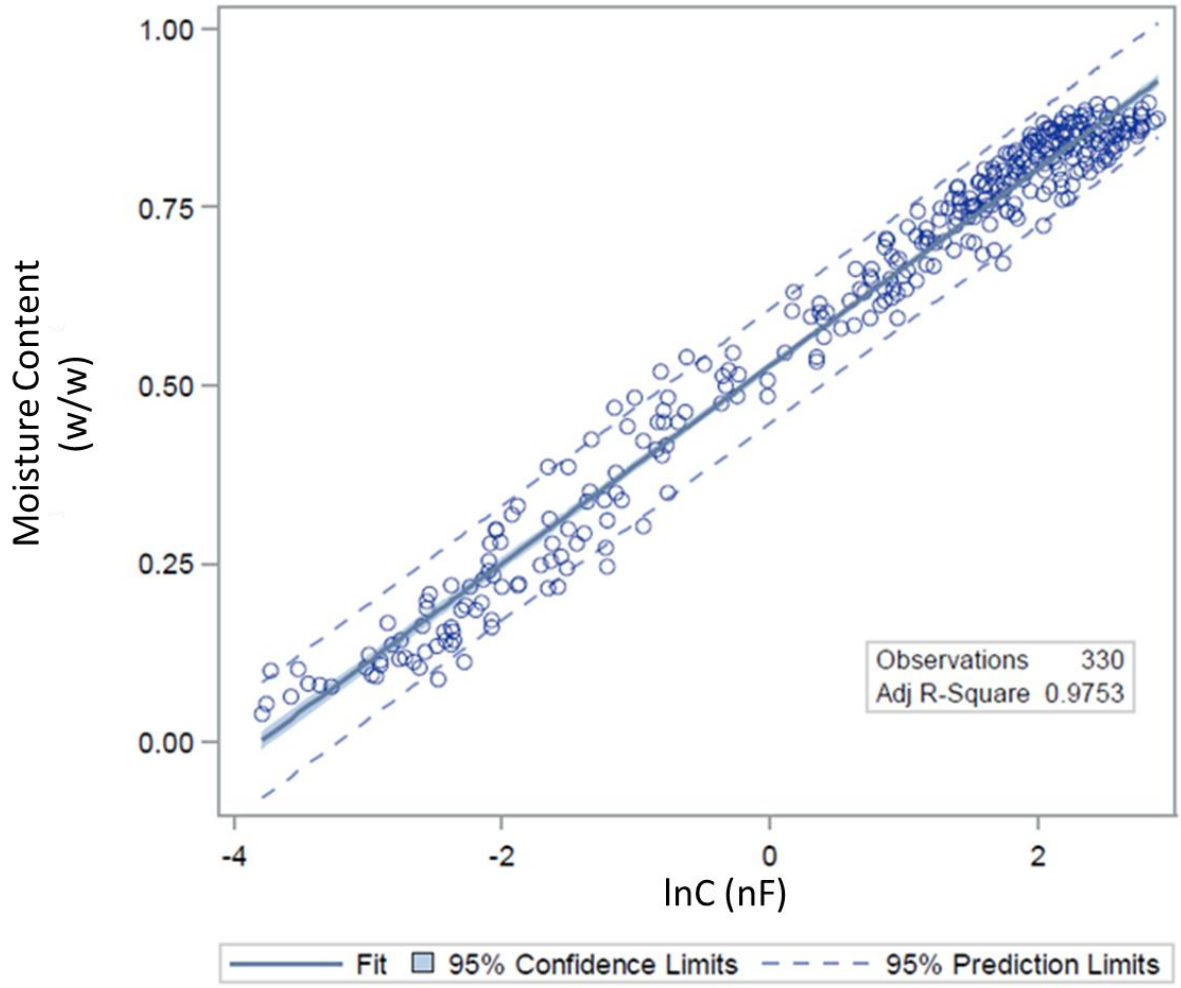

Figure 10: Illustration of the generic correlation between the natural log of capacitance and moisture content. This relationship was constructed using data from all 7 sensor geometries taken at each of the three temperatures (20 ˚C, 25 ˚C, 30˚C) sampled using a 500 Hz test signal to form a generic model.

with a 95% prediction interval of approximately ±8% moisture. Comparing individual sensors performance to that of the generic model shows that there is a marginal increase in performance from the individual sensor 1 model (figure 11).

Based on earlier finite difference method simulations, it was theorized that the changes in a and b pad dimensions would have a larger effect on sensor performance. This was not observed in prototype testing. This may become more evident when dealing with soils that are prone to shrinking and swelling more drastically than seen in testing.

Results from the soilless growth media testing showed similar results. Figure 12 displays the results of the soilless growth media testing. The watermark sensor data was measured for both capacitance and resistance and respectively explained 94% and 90% of the changes in moisture based on their independent variables. Sensor 4 and 7 were able to respectively explain 95% and 97% of the changes in moisture based on capacitance.

Conclusions and Recommendations

The moisture sensors developed and evaluated for this project were capable of measuring moisture content of wetted media by measuring changes in dielectric properties. Employing a coaxial sensor geometry to utilize capacitance mechanisms for determining moisture content proved to be a suitable option in terms of cost effectiveness, minimalizing intrusion, and

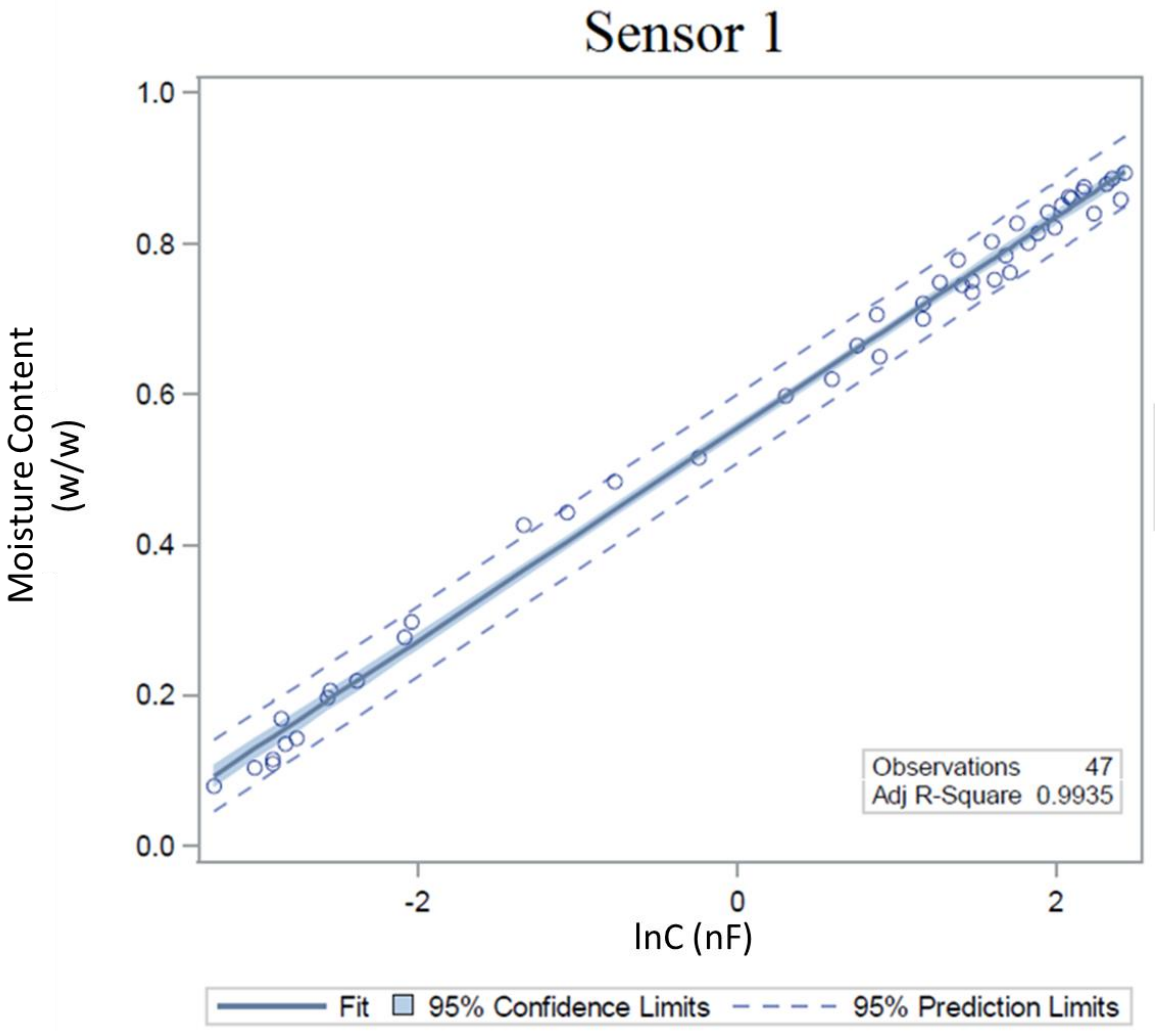

Figure 11: Illustration of the specific correlation between the natural log of capacitance and moisture content of sensor 1. This relationship was constructed using data from a single sensor geometry taken at each of the three temperatures (20 ˚C, 25 ˚C, 30˚C) sampled using a 500 Hz test signal to form a specific model.

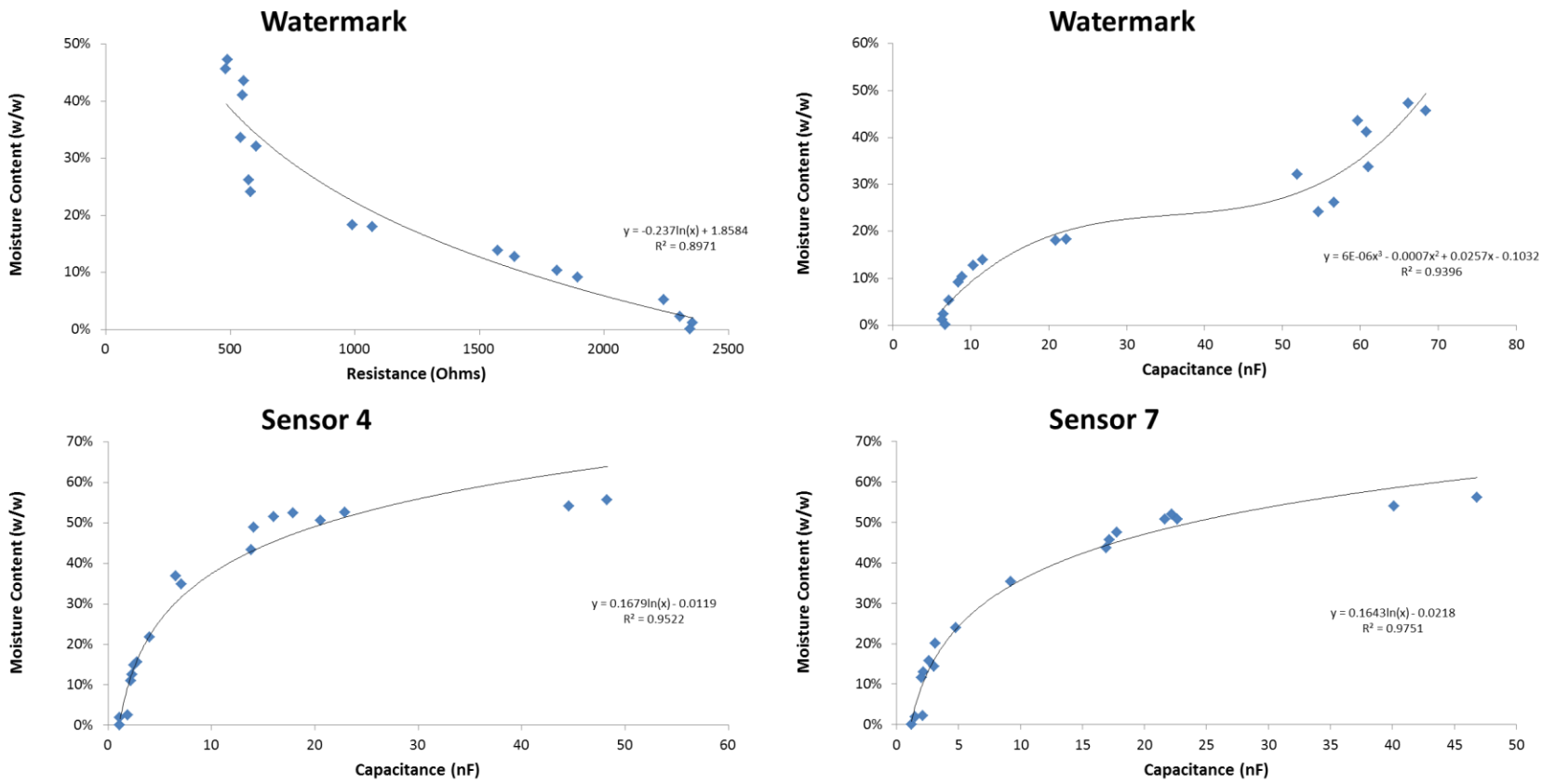

Figure 12: Results from soilless media validation testing. A negating log trend is apparent in output of the watermark sensor that correlates moisture content and resistance (top-left). A polynomial trend is apparent in output of the watermark sensor that correlates moisture content and capacitance (top-right). A positive log trend is apparent in output of both sensor 4 (bottom-left) and 7 (bottom-right) that correlates moisture content and capacitance.

simplifying implementation of the sensor. In addition, the sensor was able to accurately detect changes in soilless growing media and performed comparatively well to a commercially available soil moisture sensor, while only costing a few cents per unit to produce. The sensor provides a new cost effective tool for producers and researchers alike to monitor moisture content spatially and temporally.

While the sensor was tested using an LRC meter, that would not be an appropriate or cost effective means for field measurements. One common circuit that could be used in conjunction with a microcontroller to determine capacitance is a 555 oscillation circuit (Texas Instruments, 2015). Figure 13 illustrates an astable 555 oscillation circuit. Frequency and duty cycle of the output is directly related to resistor 1 (R1), resistor 2 (R2), and capacitor 1 (C1). The resulting output from this circuit would be in the form of a square wave (figure 14).

Charging time (t1) and discharging time (t2) can be calculated using equations 4 and 5. These t1 and t2 combine to make up the time it takes for one period (equation 6)

$$t1 = 0.693(R1 + R2) * C1 \quad (4)$$

$$t2 = 0.693 * R2 * C1 \quad (5)$$

$$T = t1 + t2 \quad (6)$$

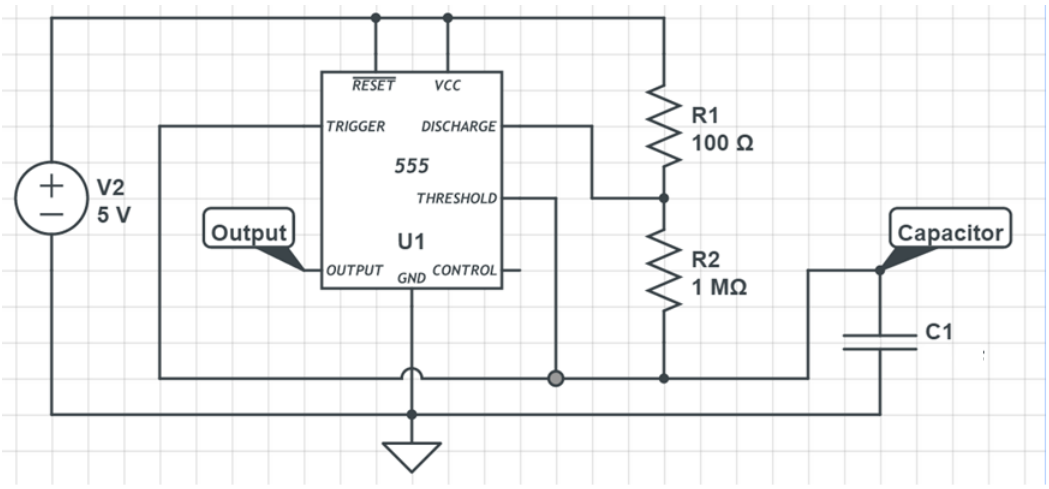

Figure 13: Illustration of an example astable oscillation circuit designed in CircuitLab. Output frequency is a function of C1, R1, and R2. With fixed resistors for R1 and R2, changes in capacitor C1 have a direct relationship to output frequency. In application C1 would be replaced with the variable capacitance moisture sensor.

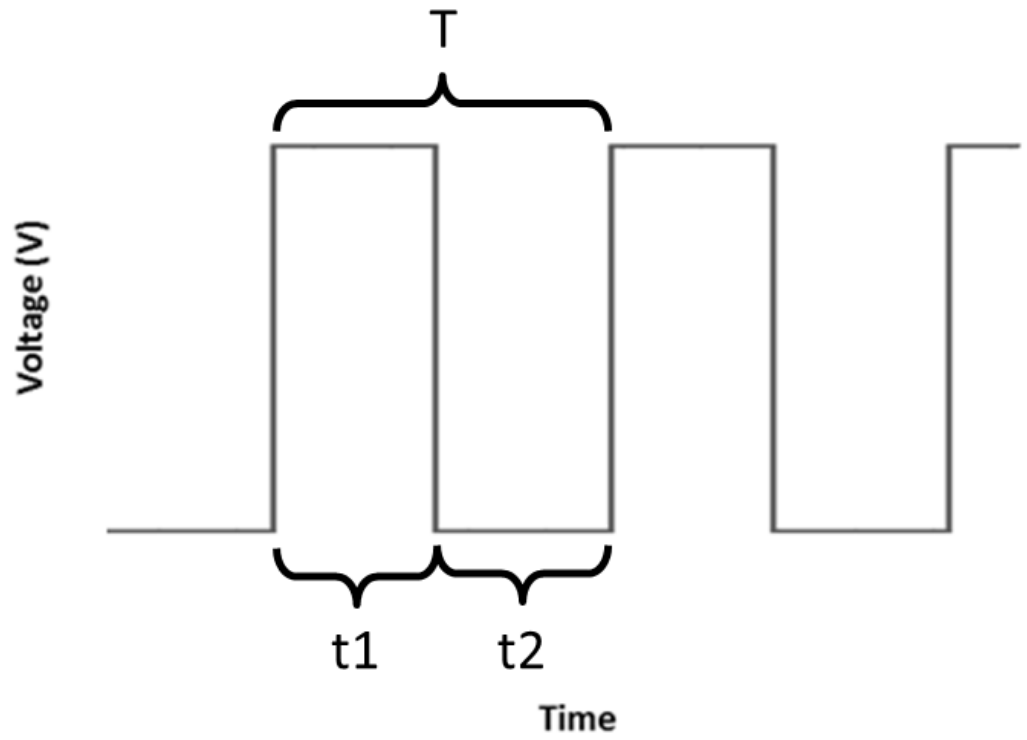

Figure 14: Illustration of sample signal output from astable oscillation circuit. The period (T) is composed of the time it takes for the leading portion of the wave (t1) and the time it takes for the trailing portion of the wave (t2).

For the example circuit in figure 13, R1 and R2 were selected to yield a duty cycle of 50% which can be calculated using equation 7. Increasing R2 decreases the duty cycle but also increases t1 and t2.

$$Duty\ Cycle = \frac{t1}{T} \quad (7)$$

Frequency (f) is the inverse of the waveform period (T). Equation 8 demonstrates this relationship.

$$f = \frac{1}{T} \quad (8)$$

A microcontroller can then be used to determine capacitance by measuring frequency of the output signal. This frequency can then be translated to capacitance with equations 4 and 5 or be related to know capacitance values empirically. Figure 15 illustrates the output signal of the previously mentioned astable circuit (figure 13) with two different capacitors to show the change in frequency.

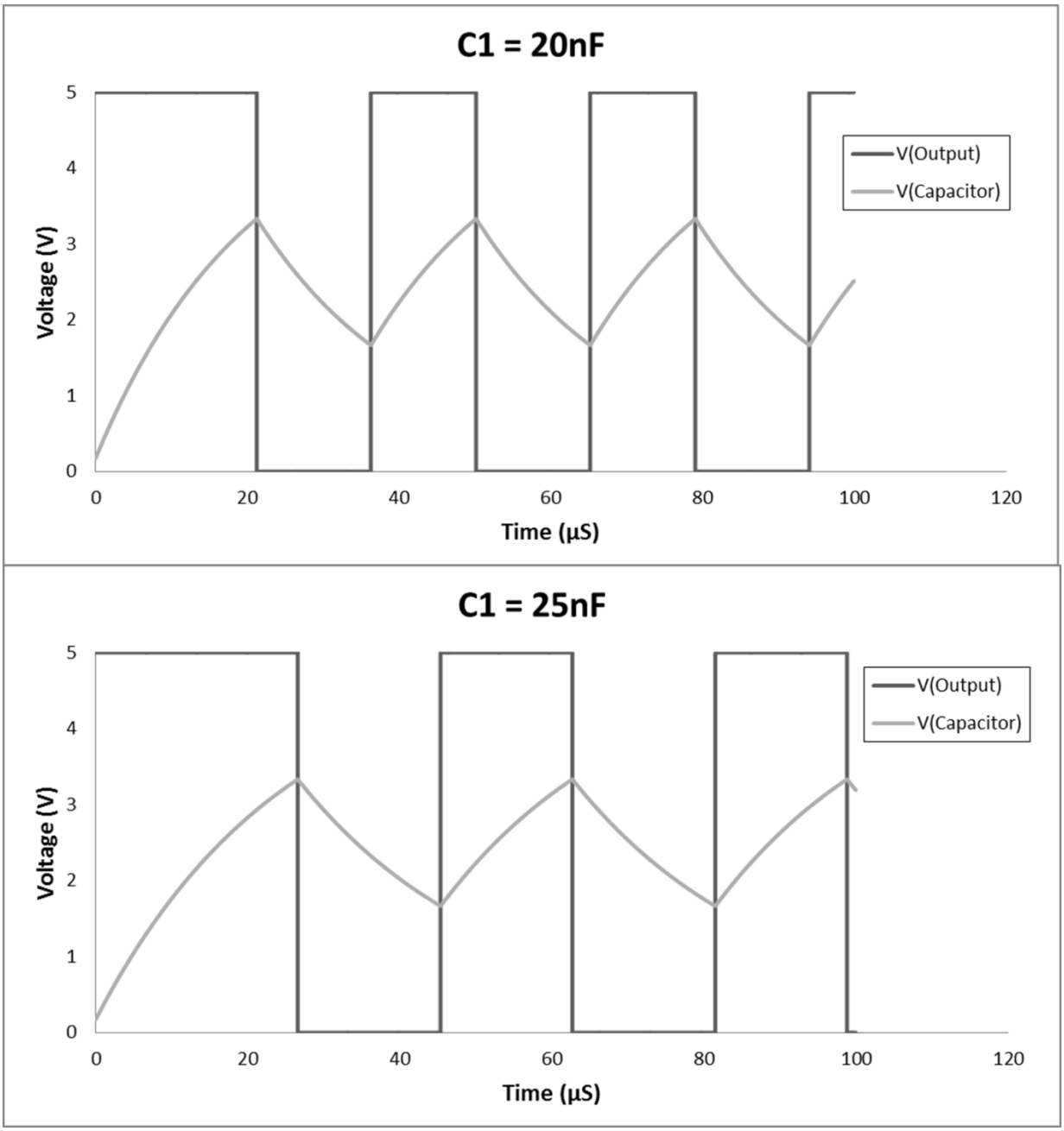

Figure 15: Illustration of the output associated with an astable circuit operated with two different capacitors inserted into C1. An increase in capacitance results in a decrease in output frequency.

CHAPTER II

Development of an Aqueous Data Transmission System for Irrigation Purposes

Abstract

Automated systems used for site specific irrigation, such as drip irrigation systems used in landscaping and greenhouses, require data transfer from multiple decentralized points to a main focal point where it is then compiled and used to make deterministic decisions based on water requirements. Automation of irrigation reduces costly input to producers and reduces the amount of highly regulated run-off caused by over irrigation. Traditional wired and wireless communication methods currently used in industry require additional infrastructure and maintenance that add to the cost of the system. The proposed aqueous data transmission system was designed to relay moisture sensor output upstream utilizing the existing irrigation infrastructure for communication. By utilizing this existing irrigation line, the system can be separated into groups. Each of the downstream assemblies, designed for transmission of sensor's data, include a microprocessor and a commonly available, variable-flow rate irrigation dripper modified to be actuated by a servomotor. Data being sent upstream is encoded by the microprocessor and transmitted by varying the flow rate at the downstream node. A pressure transducer and electronically controllable valve is employed upstream to receive data from each of the individual irrigation lines. This data is then decoded by an upstream microprocessor and used to determine the water requirement of the active node.

Introduction

Automated irrigation systems that act on environmental data require some method of communication in order to acquire sensor data from different spatial points and be able to relay that data throughout the system. Hybrid wired/wireless data transmission protocols currently available often neglect the existing infrastructure and add additional infrastructure and complexity to the irrigation system. Wireless sensor networks (WSN) have recently become a promising potential solution (Pawlowski et al., 2009). The typical arraignment of a WSN includes master nodes as well as multiple remote sensor nodes. All communication from the master node to the personal computer commonly utilizes a hard wired interface whereas the remote sensor nodes often communicate by means of a radio frequency based wireless signal. Sensor data from the remote sensor nodes are often aggregated by the master node for them to be downloaded and viewed by the end user.

Radio frequency (RF)-based wireless communication from remote sensor nodes to a master node offers many benefits including the ability to physically move each node without requiring modification to an already established network. It also offers the ability to transmit data regardless of irrigation scheduling. Drawbacks to RF-based wireless communications include power restrictions, transmission distance and line of sight through real world environments, and the added complexity of building a WSN and coupling it with the existing irrigation infrastructure. This added complexity, as well as cost, is often the deciding factor for many growers (Kelly, 2011). The proposed system offers a potential alternative to the typical RF

wireless communications protocol used for site-specific irrigation systems such as drip irrigation by utilizing the existing irrigation infrastructure. This makes it possible to simplify the setup required to implement an automated system while also retaining many of the benefits of the RF based wireless system.

Objective

In order to improve water usage efficiency in an automated site-specific irrigation system, a method for transmitting current moisture content from each site is required. The focus of this study is the development and evaluation of the aqueous data transmission concept prototype. The overall objectives for this study are:

i. To develop a method for transmitting data through an irrigation pipe filled with water,
ii. To evaluate a proof-of-concept system using commonly available drip irrigation supplies, and
iii. To demonstrate the ability of the system to transmit data through a mock irrigation system.

Design Approach

Design efforts were aimed at developing a method of transmitting data through a waterline in a fashion less susceptible to noise and other drawbacks associated with common methods of underwater communication methods like the acoustic channel. It was assumed that the Venturi effect could be used to relate pressure changes at an upstream restriction to overall flow rate. The initial concept hinged on the relationship between varying flow rate and its effects in a restricted

section of the upstream irrigation system. The relationship could be used to receive binary data from a remote irrigation point. A proof-of-concept system was constructed to test this theory and demonstrate the driving principals.

Based on literature, there was a strong likelihood of noise that could interrupt data transmission. In order to combat this, as well as the variability of system wide water demand, a tri-state communication protocol was devised. This allowed for an active high, active low and inactive state, which reduces the probability of misinterpreting received bits.

Background

While many different communication methods are currently available for the purpose transmitting data, the deciding factor in choosing between these methods is application. Typically these methods can be divided into two classifications: wired and wireless. Wired methods are best suited for long distance applications that have stable physical locations. Wireless methods are favored for scenarios that entail shorter distances but require the added flexibility of location mobility within a certain area. The majority of research on these two communication methods is concentrated on land based application. This study is primarily focused on the development of a communication protocol suited for relaying soil moisture sensor data for irrigation automation. Specifically, a sensor driven automated irrigation system using the preexisting water pipe network would take advantage of existing groundwork rather than requiring the construction of a more traditional standalone wired or wireless infrastructure. Data transmission using aqueous media filled pipes is a potentially underutilized technique in agricultural environmental sensing applications.

Underwater communication research found in published literature is mainly focused on transmitting data acoustically in open water. The underwater acoustic channel is susceptible to its own series of limitation and complications such as being reverberant (Kilfoyle and Baggeroer, 2000), prone to fading (Feder and Catipovic, 1991), and subject to multipath effects (Udahemuka, 2006). Reverberation and multipath effects are exacerbated in pipe networks making modulation and signal processing key for successful implementation of the acoustic channel. While much of the research into underwater communication has strived to increase the bit rate capability of these systems, it adds unnecessary complexity for the purpose of this study due to the limited amount of data needing to be transmitted. For this reason, a more suitable method for communicating was devised for transiting low bit rate data using a variable flow rate nozzle to modify pressure upstream.

Basic irrigation techniques, such as drip irrigation systems used in many greenhouses, set the volume of water applied to an area by selecting an irrigation nozzle with a known flow rate. These nozzles are available in both fixed and variable flow rate options. Mechanically increasing or decreasing flow rate by manipulation of the nozzle makes it is possible to vary the overall water demand in the system. Assuming incompressible fluid flow through a pipe, the continuity equation (equation 9**)** and a derivation of the Bernoulli equation (equation 10**)** can be used to calculate a change in flow rate based on a pressure differential at two points based on the Venturi effect.

$$Q = V_1 A_1 = V_2 A_2 \qquad (9)$$

$$P_1 - P_2 = \frac{\rho}{2}(V_1^2 - V_2^2) \quad (10)$$

where
Q = Flow rate through pipe ($m^3\ s^{-1}$)
V_1 = Velocity of fluid before restriction ($m\ s^{-1}$)
V_2 = Velocity of fluid at restriction ($m\ s^{-1}$)
A_1 = Cross sectional area before restriction (m^2)
A_2 = Cross sectional area at restriction (m^2)
P_1 = Pressure before restriction ($N\ m^{-2}$)
P_2 = Pressure at restriction ($N\ m^{-2}$)
ρ = Density of the fluid ($kg\ m^{-3}$)

The continuity equation dictates that with a reduction in area, velocity must increase to maintain equilibrium. In order to determine velocity, the continuity equation (equation 9**)** must be solved for unrestricted fluid velocity (V_1) as demonstrated in equation 11.

$$V_1 = V_2 \frac{A_2}{A_1} \quad (11)$$

Substituting this form of the continuity equation into equation 9 yields equation 12**,** which can be simplified to equation 13.

$$P_1 - P_2 = \frac{\rho}{2}\left[\left(V_2 \frac{A_2}{A_1}\right)^2 - V_2^2\right] \quad (12)$$

$$P_1 - P_2 = \frac{\rho V_2^2}{2}\left[\left(\frac{A_2}{A_1}\right)^2 - 1\right] \quad (13)$$

With an increase in overall flow rate (Q), a resulting increase in velocity (V1 and V2) will occur according to the continuity equation (equation 9**)**. This will result in an increase in the pressure differential (P1-P2) between the unrestricted cross sectional area (A1) and the restricted cross

sectional area (A2) based on equation 13. Figure 16 is an illustration of these variables and their relation to each other for reference.

Materials and Methods

System components used in testing can be broken down into either irrigation or electronic-based components. All drip irrigation supplies were sourced from a local home improvement store. The only component used in the design of the system not commercially available is the valve actuators used for automating control of the variable flow rate nozzles.

Experimental Design

A small scale irrigation system was constructed for the purpose of testing the prototype communication method. The transmitting system was programed to send a single packet of data which consisted of 9 bits. The receiving system recorded pressure continuously, and this data was stored on a personal computer for post processing in Excel for analysis and verification.

Methods

The transmission method was evaluated by assembling a prototype irrigation system outfitted with electronics for transmitting and receiving data through the water line. While designing a drip irrigation system was not a direct objective of this study, it was necessary for testing purposes.

Irrigation components (fittings, adapters, regulators, drippers) used in the construction of the prototype system were drip irrigation supplies commonly sourced from local home improvement

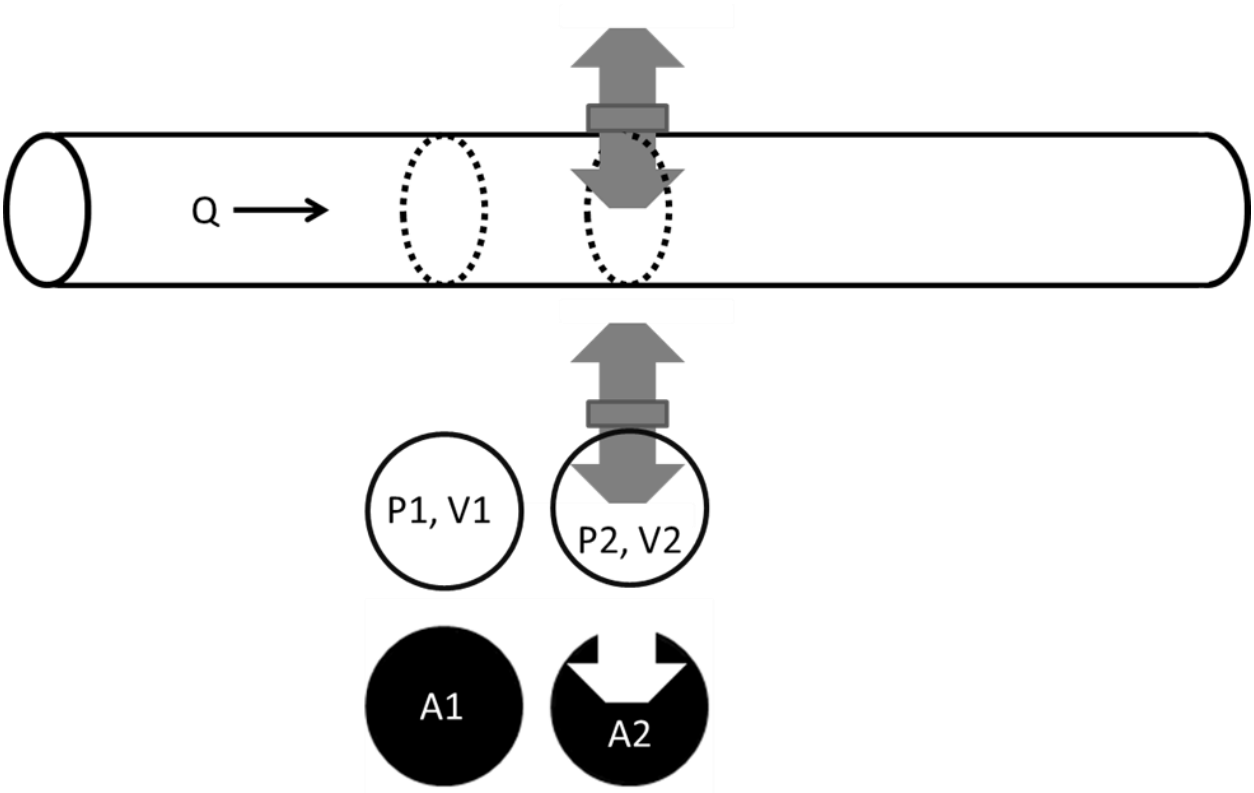

Figure 16: Illustration of pipe flow variables associated with Venturi calculations. As area decreases from A1 to A2, pressure at the restriction (P2) is decreased while velocity (V2) is increased compared to their corresponding upstream parameters (P1, V1).

stores. A drip irrigation style system was selected for testing for the because of its widespread usage in both commercial and non-commercial industries. Pressure of the system was controlled with a fixed 25 psi pressure regulator. The irrigation lines were configured as illustrated in figure 17. The backbone of the system was a one inch polyethylene distribution tubing. Three ¼" vinyl remote irrigation tubes were joined to the distribution tube with barb fittings. Each of the three ¼" vinyl lines was further divided, using T-fittings, to supply irrigation to a fixed flow dripper and a modified adjustable flow rate dripper.

Electric components can be further sub-divided into either components used for transmitting (TX) or components used for receiving data (RX). A block diagram of both systems is illustrated in figure 18. Both TX and RX systems contained a micro controller (Arduino Uno) responsible for their individual programmed tasks. During testing, both systems were operated continuously negating the requirement of a clock.

The TX system was located at the emission point of the irrigation system. A modified adjustable flow dripper was used for transmitting. This dripper was built with a servo (Hitec HS-82MG) that was used to actuate the dripper with an adjustable linkage. This allowed for automated manipulation of flow rate. Figure 19 shows one of the modified drippers for reference. An arbitrary method for frequency modulation was devised for testing purposes. A 40-degree rotation of the adjustable dripper flow valve followed by a delay was used to represent a binary "0". This sequence was repeated twice in order to represent a binary "1".

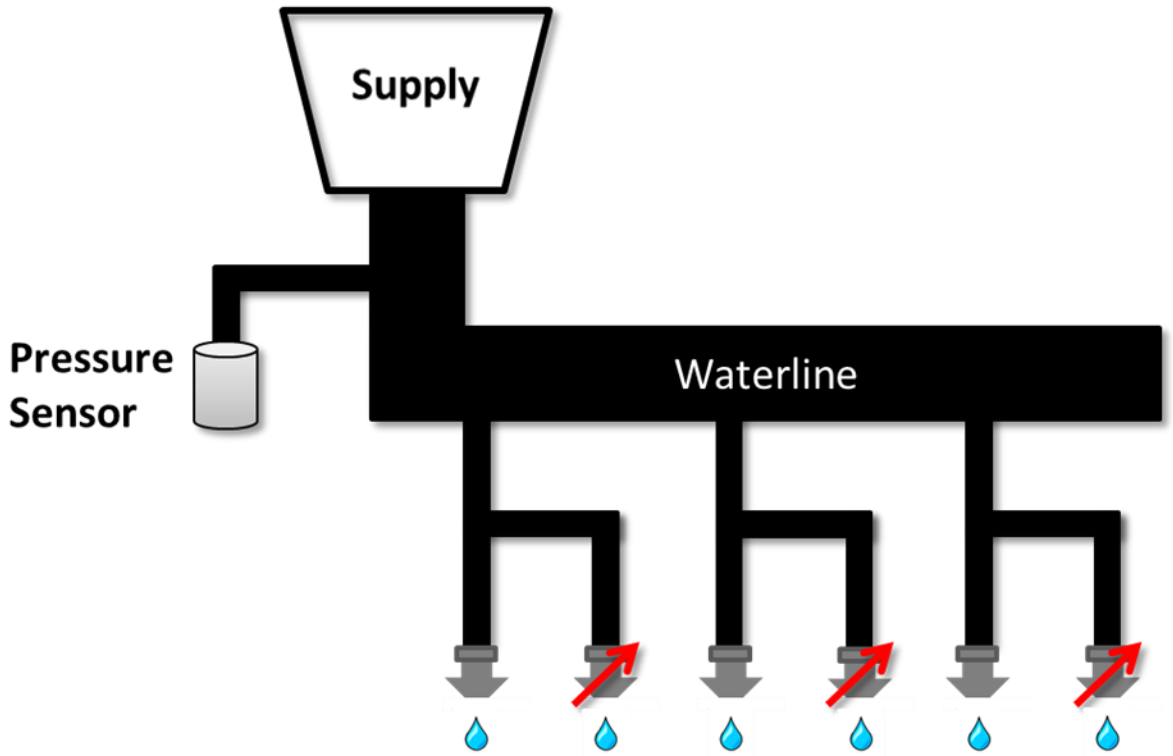

Figure 17: Illustration of mock irrigation system layout used for testing. Drippers with arrows through them indicate modified variable drippers for output of data. An upstream pressure sensor is used for input of data through the waterline.

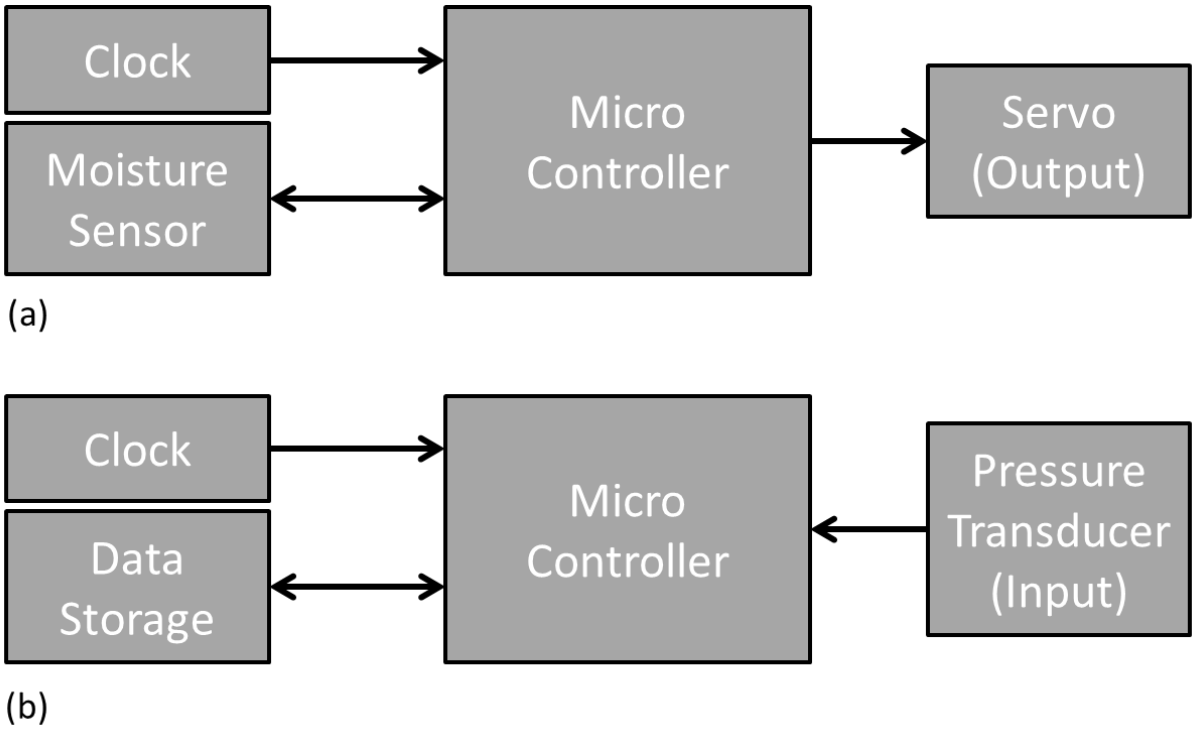

Figure 18: Block diagram of electronic sub-systems. (a) Moisture measurements are transmitted through the system with a variable dripper valve actuated by a micro controller automated servo. (b) Moisture measurements are received upstream through a pressure transduced and relayed to a storage sub-system by a second micro controller.

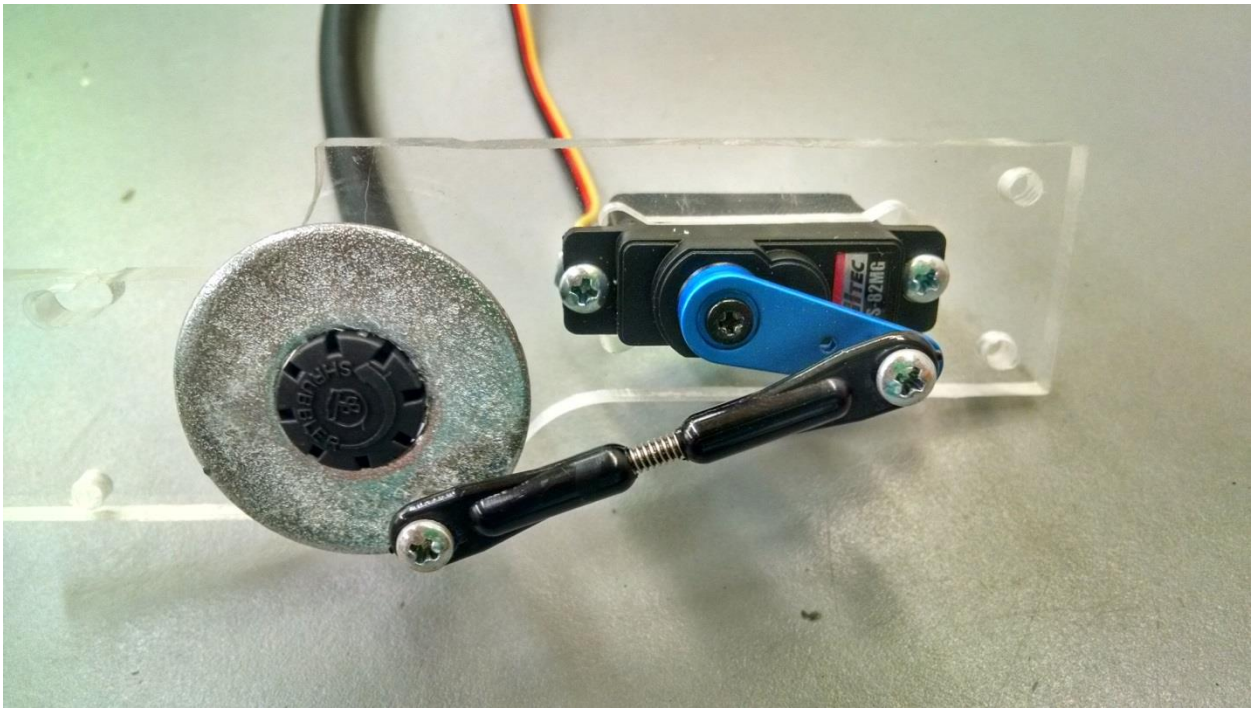

Figure 19: Photograph of a modified adjustable flow dripper. A servo is attached to a variable dripper by means of a spherical bearing linkage allowing for the automated actuation of the dripper.

The RX system, located near the main water supply, monitored pressure and relayed this data to personal computer serially for local storage. System pressure was sensed with a transducer (Honeywell NBPDANN150PGUNV). This sensor was connected to the main irrigation polyethylene tube via a ¼" line filled with air to protect the sensor. Code for both the TX and RX system micro controllers can be found in appendix B

Measurements

Air was purged from the system. A series of 4 data packets containing 8 bits (32 bits total) were transmitted through the waterline over a 5 minute period at approximately 0.1 bits per second. Each of the 4 data packets contained a 3 bit start sequence of "111" followed by five random bits. The data packets were recorded for verification of output data. Pressure was recorded continuously during testing and transmitted to a connected PC serially for analysis and verification against the sent packets.

Results and Discussion

Data packet tests were conducted in order to ascertain an appropriate delay in servo dripper timing that optimized bit rate and data success rate. Data was recorded and transmitted to a connected PC. The derivative of the raw data was taken in order to find the slope at each data point. Slope was categorized as being either positive or negative. Sections with positive slope indicated an increase in pressure and the timing of these events dictated the binary value of the bit. Long periods of time with increases in pressure were representative of the binary digit 1 while short periods of time with increases in pressure were the digit 0. Figure 20 shows the raw

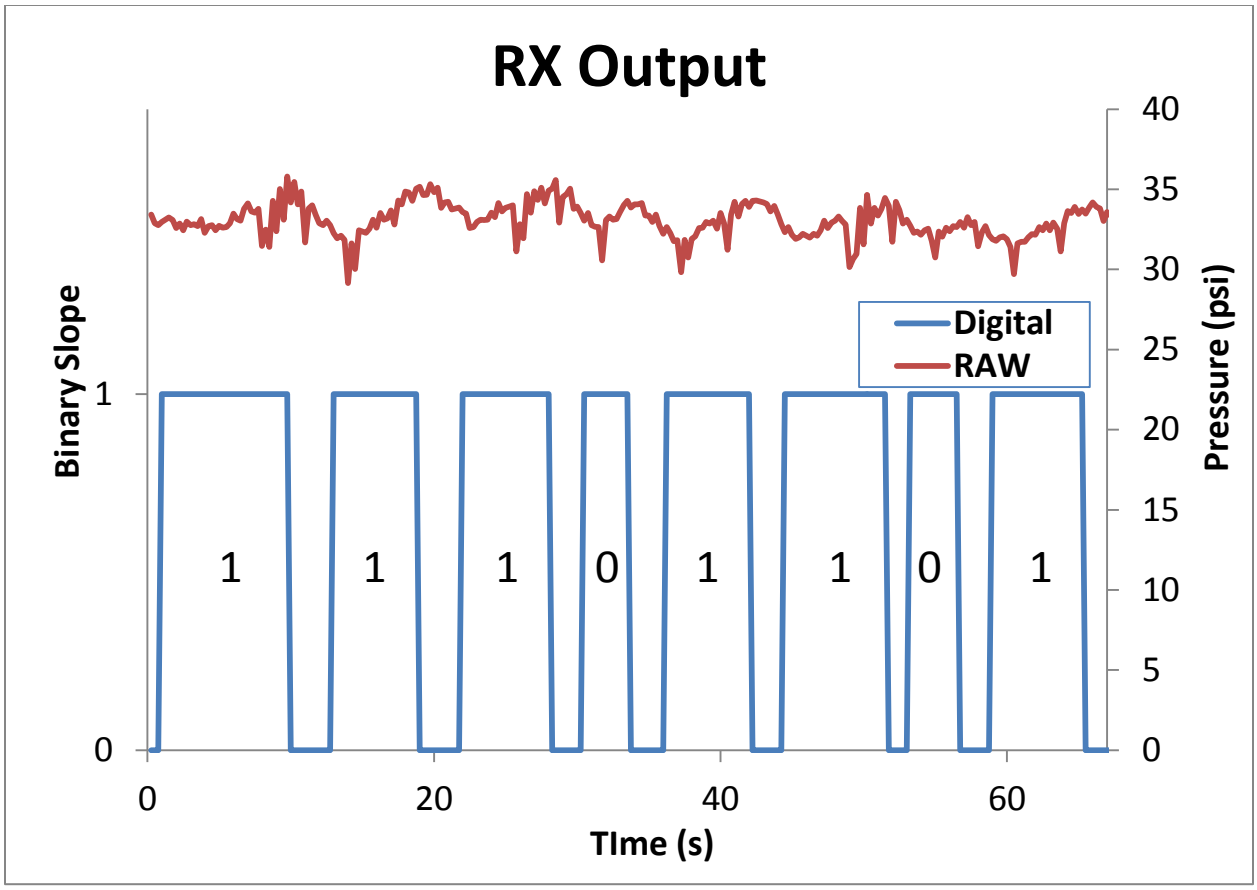

Figure 20: Output from sample 8 bit packet test. Raw pressure data (top) corresponds with the right y-axis while demodulated binary output (bottom) corresponds with the left y-axis. Long time periods of positive slope in the raw signal are interpreted as a binary 1 while short time periods of positive slope represent a binary 0.

pressure data of one packet (8 bits) contained in the 4 packet transmission test. The packet of data was successfully demodulated and the resulting digital signal can be seen graphed as well. Figure 21 shows a graph of a full data packet test conducted over a period of five minutes. Once appropriate timing was established, the data packet test was conducted 10 times.

Conclusion and Recommendations

The aqueous data transmission system was capable of reliably sending information over a network of irrigation tubing. Once sufficient timing was provided, all 32 were reliably received and demodulated correctly during data packet testing. One drawback of the system was the transmission speed. While this was a predicted drawback from the beginning it's a limiting factor worth expanding upon. In order to get adequate separation between bits a large amount of delay was required for pressure changes to equalize in the system. A bit rate of 0.1 bits per second was achieved during testing. This didn't pose a problem since only 32 bits of data were being transmitted. Data packet testing took approximately 5 minutes to transmit 32 bits of data. This would become more evident as the amount of data increased. These results allowed for the following conclusion:

- The data transmission system was capable of achieving 0.1 bps and accurately transmitted data at this bite rate
- Multiple active drippers had no ill effects on the ability to transmit data through the network
- The system was able to asynchronously transmit over 5 minutes without error

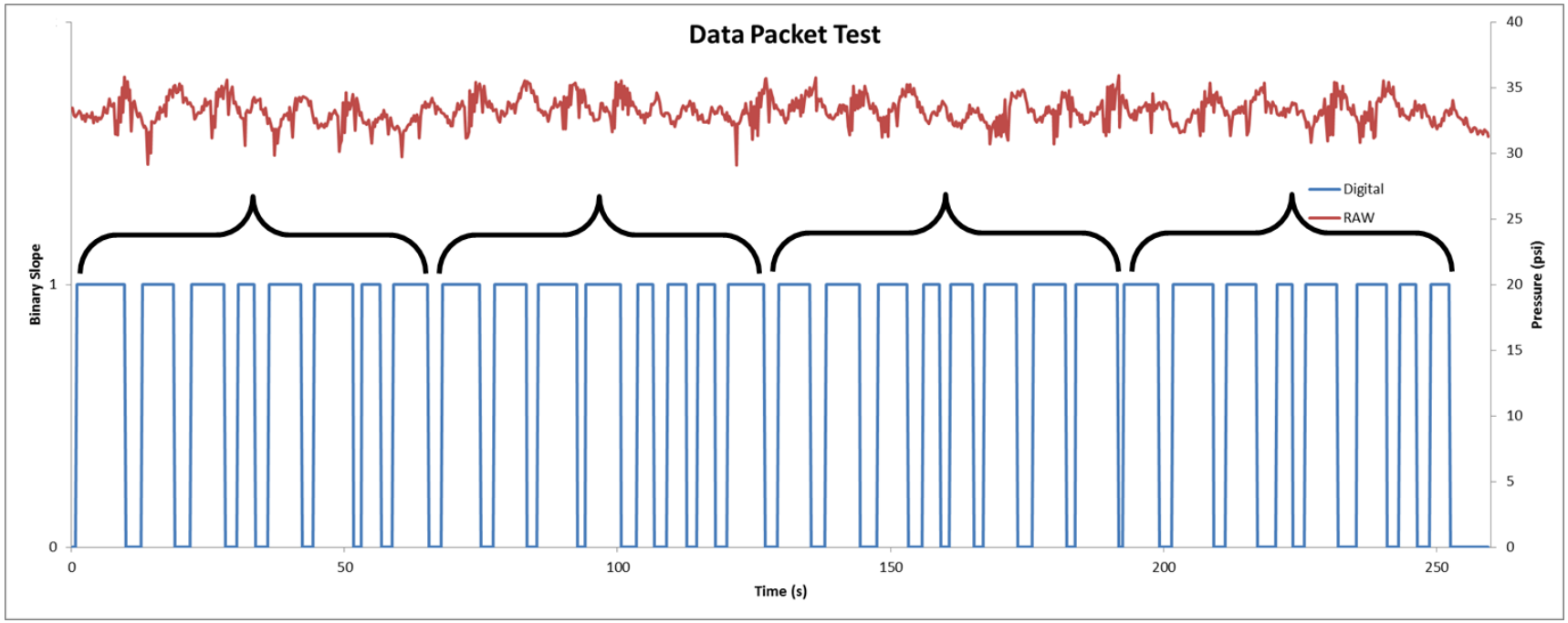

Figure 21: Output from 32 bit (4 packets) data transmission test. Each of the 4 packets is grouped within a bracket. Raw pressure data (top) corresponds with the right y-axis while demodulated binary output (bottom) corresponds with the left y-axis. Long time periods of positive slope in the raw signal are interpreted as a binary 1 while short time periods of positive slope represent a binary 0.

CONCLUSION

The development and evaluation of a cost effective plant growth media a moisture sensor for site specific irrigation automation has been discussed in Chapter I of this thesis. In addition, the development of an aqueous communication method for transmitting data through a network of fluid filled pipes in an irrigation system has been discussed in Chapter II. Combined, these two components make up a system that has the ability to monitor spatial differences in moisture and transmit this data back to a centralized location for the purpose of automated irrigation and historical modeling. Each chapter detailed the development of a system, the testing of that system, and then the optimization of that system. The results of this allowed for the following conclusions:

- The moisture sensors were effective at measuring moisture content in the surrounding media within ±5% compared to gravimetric measurements.
- The PCB Planar-coaxial capacitor design provided a cost effective method of measuring soil moisture compared to commercially available options.
- The data transmission method was capable of transmitting 100% of data though irrigation tubing.
- The implementation of frequency modulation base on the leading edge of pressure increases reduced the otherwise significant impact of system noise.

REFERENCES

Aspinall, D., P. Nicholls, and L. May. 1964. The effects of soil moisture stress on the growth of barley. I. Vegetative development and grain yield. Crop and Pasture Science 15(5):729-745.

Bhatti, M., and J. Kraft. 1992. Influence of soil moisture on root rot and wilt of chickpea. Plant disease 76(12):1259-1262.

Christian-Smith, J., and P. H. Gleick. 2012. A twenty-first century US water policy. Oxford University Press.

Coleman, P., L. Ellerbrock, and J. Lorbeer. 1992. Interaction of Phoma terrestris and soil moisture level on yield of two onion cultivars differentially susceptible to pink root. Plant disease 76(12):1213-1216.

Dean, T., J. Bell, and A. Baty. 1987. Soil moisture measurement by an improved capacitance technique, Part I. Sensor design and performance. Journal of Hydrology 93(1):67-78.

Denmead, O., and R. H. Shaw. 1960. The effects of soil moisture stress at different stages of growth on the development and yield of corn. Agronomy Journal 52(5):272-274.

Feder, M., and J. A. Catipovic. 1991. Algorithms for joint channel estimation and data recovery-application to equalization in underwater communications. IEEE Journal of Oceanic Engineering 16(1):42-55.

Hasted, J. B. 1973. Aqueous dielectrics. Chapman and Hall.

Kelly, C. M. 2011. Development of an environmental monitoring system for greenhouse disease management. MS Thesis. University of Tennessee, Biosystems Engineering, Knoxville Tennessee.

Kilfoyle, D. B., and A. B. Baggeroer. 2000. The state of the art in underwater acoustic telemetry. IEEE Journal of Oceanic Engineering 25(1):4-27.

Krupinsky, J. M., K. L. Bailey, M. P. McMullen, B. D. Gossen, and T. K. Turkington. 2002. Managing plant disease risk in diversified cropping systems. Agronomy Journal 94(2):198-209.

Leib, B. G., J. D. Jabro, and G. R. Matthews. 2003. Field evaluation and performance comparison of soil moisture sensors. Soil Science 168(6):396-408.

Nemali, K. S., and M. W. van Iersel. 2006. An automated system for controlling drought stress and irrigation in potted plants. Scientia horticulturae 110(3):292-297.

Patz, J. A. 1998. Predicting key malaria transmission factors, biting and entomological inoculation rates, using modelled soil moisture in Kenya. Tropical Medicine & International Health 3(10):818-827.

Pawlowski, A., J. L. Guzman, F. Rodríguez, M. Berenguel, J. Sánchez, and S. Dormido. 2009. Simulation of greenhouse climate monitoring and control with wireless sensor network and event-based control. Sensors 9(1):232-252.

Ranganath, P. 2013. Electric field of a parallel plate capacitor using 2D poisson equation. Available at: http://www.mathworks.com/matlabcentral/fileexchange/42773-electric-field-of-a-parallel-plate-capacitor-using-2d-poisson-equation.

Sadiku, M. 2014. Elements of electromagnetics (the oxford series in electrical and computer engineering). Oxford University Press, USA.

Sherfy, A. C. 2008. Assembly and evaluation of a multi-functional heat pulse probe for measurement of soil properties. MS Thesis. University of Tennessee, Environmental and Soil Science, Knoxville Tennessee.

Texas Instruments. 2015. LM555 timer data sheet. Available at: http://www.ti.com/lit/ds/symlink/lm555.pdf.

Udahemuka, G. 2006. Digital communication over a water pipe network. Tshwane University of Technology.

Walker, J. P., G. R. Willgoose, and J. D. Kalma. 2004. In situ measurement of soil moisture: a comparison of techniques. Journal of Hydrology 293(1):85-99.

Whalley, W., T. Dean, and P. Izzard. 1992. Evaluation of the capacitance technique as a method for dynamically measuring soil water content. Journal of agricultural engineering research 52:147-155.

WHO. 2013. World malaria report 2013. World Health Organization Press:62-63.

Zazueta, F. S., and J. Xin. 1994. Soil moisture sensors. Soil Science 73:391-401.

APPENDIX

Appendix A – Modified MATLAB Code for Thin Coaxial Capacitors

```
%-------------------------------------------------------------------------%
%  This simple program computes the Electric Fields due to
%  Parallel plate Capacitors using the Finite difference method (FDM)
%-------------------------------------------------------------------------%

clc
close all; clear all;

%-------------------------------------------------------------------------%
%                SYMBOLS USED IN THIS CODE
%-------------------------------------------------------------------------%

% E = Total electric field matrix using Poisson's equation
% V = Potential matrix
% Nx = Number of grid points in X- direction
% Ny = Number of grid points in Y-Direction
%-------------------------------------------------------------------------%


%-------------------------------------------------------------------------%
%                     INITIALIZATION
%         Here, all the grid, size, charges, etc. are defined
%-------------------------------------------------------------------------%

% Enter the dimensions

Nx = 101;     % Number of X-grids
Ny = 101;     % Number of Y-grids
mpx = ceil(Nx/2); % Mid-point of x
mpy = ceil(Ny/2); % Mid point of y


Ni = 750;  % Number of iterations for the Poisson solver

V = zeros(Nx,Ny);   % Potential (Voltage) matrix

T = 0;          % Top-wall potential
B = 0;          % Bottom-wall potential
L = 0;          % Left-wall potential
R = 0;          % Right-wall potential

%-------------------------------------------------------------------------%
% Initializing edges potentials
%-------------------------------------------------------------------------%

V(1,:) = L;
V(Nx,:) = R;
V(:,1) = B;
V(:,Ny) = T;

%-------------------------------------------------------------------------%
% Initializing Corner potentials
%-------------------------------------------------------------------------%
```

```
V(1,1) = 0.5*(V(1,2)+V(2,1));
V(Nx,1) = 0.5*(V(Nx-1,1)+V(Nx,2));
V(1,Ny) = 0.5*(V(1,Ny-1)+V(2,Ny));
V(Nx,Ny) = 0.5*(V(Nx,Ny-1)+V(Nx-1,Ny));

%------------------------------------------------------------------------%


length_plate = 51;  % Length of plate in terms of number of grids
lp = floor(length_plate/2);

position_plate = 15; % Position of plate on x axis
pp1 = mpx;%mpx+position_plate;
pp2 = mpx;%mpx-position_plate;

for z = 1:Ni    % Number of iterations

      i=(2:Nx-1);
      j=(2:Ny-1);

         % The next two lines are meant to force the matrix to hold the
         % potential values for all iterations

            V(pp1,mpy:mpy+20) = -3;
            V(pp2,mpy-40:mpy-10) = 3;
            V(mpx-20:mpx-10,mpy-20:mpy-10)=0;

            %Jacobi's iterative method http://www.physics.buffalo.edu/phy410-505/2011/topic3/app1/index.html
            V(i,j)=0.25*(V(i+1,j)+V(i-1,j)+V(i,j+1)+V(i,j-1));



end

% Take transpose for proper x-y orientation
V = V';

[Ex,Ey]=gradient(V);
Ex = -Ex;
Ey = -Ey;



% Electric field Magnitude
 E = sqrt(Ex.^2+Ey.^2);

x = (1:Nx)-mpx;
y = (1:Ny)-mpy;

% Contour Display for electric potential
figure(1)
contour_range_V = -101:0.5:101;
contour(x,y,V,contour_range_V,'linewidth',0.5);
axis([min(x) max(x) min(y) max(y)]);
colorbar('location','eastoutside','fontsize',14);
xlabel('x-axis in meters','fontsize',14);
```

```
ylabel('y-axis in meters','fontsize',14);
title('Electric Potential distribution, V(x,y) in volts','fontsize',14);
h1=gca;
set(h1,'fontsize',14);
fh1 = figure(1);
set(fh1, 'color', 'white')


% Contour Display for electric field
figure(2)
contour_range_E = -20:0.05:20;
contour(x,y,E,contour_range_E,'linewidth',0.5);
axis([min(x) max(x) min(y) max(y)]);
colorbar('location','eastoutside','fontsize',14);
xlabel('x-axis in meters','fontsize',14);
ylabel('y-axis in meters','fontsize',14);
title('Electric field distribution, E (x,y) in V/m','fontsize',14);
h2=gca;
set(h2,'fontsize',14);
fh2 = figure(2);
set(fh2, 'color', 'white')

% Quiver Display for electric field Lines
figure(3)
contour(x,y,E,'linewidth',0.5);
hold on, quiver(x,y,Ex,Ey,2)
title('Electric field Lines, E (x,y) in V/m','fontsize',14);
axis([min(x) max(x) min(y) max(y)]);
colorbar('location','eastoutside','fontsize',14);
xlabel('x-axis in meters','fontsize',14);
ylabel('y-axis in meters','fontsize',14);
h3=gca;
set(h3,'fontsize',14);
fh3 = figure(3);
set(fh3, 'color', 'white')


%------------------------------------------------------------------------%
% REFERENCE
%         SADIKU, ELEMENTS OF ELECTROMAGNETICS, 4TH EDITION, OXFORD
%------------------------------------------------------------------------%
```

Appendix B – Arduino Code for TX and RX systems

```
// SweepREADarray
// by Steven Pickett
// This example code is in the public domain.


#include <Servo.h>
#include <TimerOne.h>

Servo myservo;  // create servo object to control a servo

byte testA[4][8]={
  {1,1,1,0,1,1,0,1},
  {1,1,1,1,0,0,0,1},
  {1,1,1,0,0,1,1,1},
  {1,1,1,0,1,1,0,0}
};

int pos = 0;    // variable to store the servo position
int row = 0;    // variable to store the row position
int col = 0;    // variable to store the column position

const int analogInPin = A0;    // Analog input pin of pressure transducer
float sensorValue = 0;                          //value read from the pot
float voltage = 0;
float psi = 0;

int x = 2500;




void setup()
{
  myservo.attach(18);  // attaches the servo on pin 18 to the servo object

  Serial.begin(9600);

  Timer1.initialize(250000);
  Timer1.attachInterrupt(READ); // Run the READ subprogram every 250ms
}


void loop()
{
  delay(5000);

  for(row = 0; row < 4; row += 1) //Grab the first row
  {

    for(col = 0; col < 8; col += 1) //Read off each digit
    {
     //decide what to do with the digit
      if (testA[row][col] == 0)
```

```
    {
      //Serial.println("Short");
      SHORT();
    }

    else if (testA[row][col] == 1)
    {
      //Serial.println("Long");
      LONG();
    }

    else
    {
      Serial.println("Invalid Input");
    }

   }

   //Serial.println();
  }

  HOLD();
}

//subprograms-----------------------------------------------------------------------

void SHORT(void)
{
  for(pos = 70; pos < 110; pos += 2)  // goes from 70 degrees to 110 degrees
  {                                   // in steps of 2 degree
    myservo.write(pos);               // tell servo to go to position in variable 'pos'
    delay(15);                        // waits 15ms for the servo to reach the position
  }

  delay(x);                           //wait for pressure to ramp up

  for(pos = 110; pos > 70; pos -= 2)  // goes from 110 degrees back to 70 degrees
  {                                   // in steps of 2 degree
    myservo.write(pos);               // tell servo to go to position in variable 'pos'
    delay(15);                        // waits 15ms for the servo to reach the position
  }
  delay(x);                           //wait for pressure to ramp down
}

void LONG(void)
{
  for(pos = 70; pos < 110; pos += 2)  // goes from 70 degrees to 110 degrees
  {                                   // in steps of 2 degree
    myservo.write(pos);               // tell servo to go to position in variable 'pos'
    delay(15);                        // waits 15ms for the servo to reach the position
  }

  delay(x);                           //wait for pressure to ramp up

  for(pos = 110; pos < 150; pos += 2)  // goes from 110 degrees to 150 degrees
  {                                   // in steps of 2 degree
    myservo.write(pos);               // tell servo to go to position in variable 'pos'
```

```
   delay(15);                       // waits 15ms for the servo to reach the position
  }
  delay(x);                         //wait for pressure to ramp up...some more

   for(pos = 150; pos > 70; pos -= 2)  // goes from 150 degrees to 70 degrees
  {                                 // in steps of 1 degree
   myservo.write(pos);              // tell servo to go to position in variable 'pos'
   delay(15);                       // waits 15ms for the servo to reach the position
  }
  delay(x);                         //wait for pressure to ramp down
}

void READ(void)
{
  sensorValue = analogRead(analogInPin);                  //read the pressure
  delay(100);                                             //hang on for a sec
  sensorValue = sensorValue + analogRead(analogInPin);      //read the pressure...again. Add it to the old pressure reading

  sensorValue = sensorValue/2;       //Average the two. Shouldnt be much change but if there is this cuts it in half.

  voltage = 5*(sensorValue/1024);    // analogREAD gives output 0-1023 relating to 0 - 5v on input
  psi = 0.0631*sensorValue - 2.3805; //found experimentally with analog pressure guage

  Serial.print("Voltage = " );
  Serial.print(voltage);
  Serial.print("v\t Pressure = ");
  Serial.println(psi);

}

void HOLD(void)
{

  delay(1000000000);
}
```

VITA

Steven M. Pickett was born October 23rd, 1985 in Cookeville, Tennessee. He was raised in Alcoa, Tennessee where he attended Alcoa Elementary School and Alcoa Middle School. He started his high school career at Alcoa High School and graduated from Knoxville Catholic High School. In August of 2004 he began attending the Tennessee Technology University in Cookeville. While at TTU, he was involved in the marching band and was a member of the Beta Thea Pi fraternity. In December of 2006 he moved back to Alcoa and began attending Pellissippi State Technical Community College while training for management with RadioShack. He graduated in May of 2009 with an Associates of Science degree with a focus on Civil Engineering. He accepted a management position with RadioShack until January of 2010 when he began attending the University of Tennessee. While at UT, he served as an Ambassador to the College of Agriculture. Steven was fortunate enough to hold internships with DuPont Danisco Cellulosic Ethanol and Oak Ridge National Laboratory during his undergraduate career. He graduated in May of 2012 with a Bachelor's degree in Biosystems Engineering. He began perusing his Master of Science degree in Biosystems Engineering in August of 2012. During his first year of graduate school he was employed by the College of Engineering as a Graduate Teaching Assistant, teaching a course in the Engineering Fundamentals department.